Standard model tests with trapped radioactive atoms

2009 J. Phys. G: Nucl. Part. Phys. 36 033101

(http://iopscience.iop.org/0954-3899/36/3/033101)

J. Phys. G: Nucl. Part. Phys. **36** (2009) 033101 (38pp) doi:10.1088/0954-3899/36/3/033101

TOPICAL REVIEW

Standard model tests with trapped radioactive atoms

J A Behr[1] **and G Gwinner**[2]

[1] TRIUMF, 4004 Wesbrook Mall, Vancouver, British Columbia V6T 2A3, Canada
[2] Department of Physics and Astronomy, University of Manitoba, Winnipeg, Manitoba R3T 2N2, Canada

E-mail: behr@triumf.ca and gwinner@physics.umanitoba.ca

Received 23 October 2008
Published 10 February 2009
Online at stacks.iop.org/JPhysG/36/033101

Abstract

We review the use of laser cooling and trapping for Standard Model tests, focusing on trapping of radioactive isotopes. Experiments with neutral atoms trapped using modern laser-cooling techniques are testing several basic predictions of electroweak unification. For nuclear β decay, demonstrated trap techniques include neutrino momentum measurements from beta-recoil coincidences, along with methods to produce highly polarized samples. These techniques have set the best general constraints on non-Standard Model scalar interactions in the first generation of particles. They also have the promise to test whether parity symmetry is maximally violated, to search for tensor interactions, and to search for new sources of time-reversal violation. There are also possibilities for exotic particle searches. Measurements of the strength of the weak neutral current can be assisted by precision atomic experiments using traps loaded with small numbers of radioactive atoms, and sensitivity to possible time-reversal violating electric dipole moments can be improved.

(Some figures in this article are in colour only in the electronic version)

1. Introduction

This paper will review experiments testing symmetries of the Standard Model (SM) of particle physics by laser trapping and cooling neutral atoms. The atom traps make possible new experiments to study an old problem, nuclear β decay. The laser cooling and trapping techniques also enable precision atomic measurements, with the possibility of practical experiments with inherently small amounts of radioactive isotopes where symmetry-violating effects are enhanced. Previous reviews of the subject include [1].

It is beyond our scope to cover interesting experiments in weak interactions with ion traps. Ongoing beta–neutrino (β–ν) correlation experiments include measuring the daughter recoil

momentum with a Penning trap [2], β^--recoil coincidences with a Paul trap [3], and other neutrino-induced kinematic shifts in a Paul trap [4].

1.1. The electroweak interaction: what we think we know

There are several basic features of electroweak unification that trap experiments can test. The photon has 'heavy light' boson partners W^+, W^- and Z^0 which mediate the weak interaction. These are all spin-1 'vector' bosons, which immediately implies that the Lorentz transformation properties of the effective low-energy four-Fermion contact operators are vector and axial vector. Measurements using atom traps have constrained other interactions by improved measurements of the historically valuable β–ν correlation.

For reasons that are not completely understood, the weak interaction is phenomenologically completely 'chiral': it only couples to left-handed neutrinos, and parity is maximally violated. The first experiments using the β-decay of laser-cooled polarized atoms have been completed, and there is promise for them to compete with and complement precision measurements of neutron β decay.

The neutral weak coupling of the Z^0 is predicted from the other couplings. At momentum transfer much less than the Z^0 production, this has been best tested in cesium atomic parity violation using thermal atomic beams [5] and in intermediate energy Møller scattering at SLAC [6]. Atoms with larger atomic number Z have larger electron wavefunction overlap with the nucleus, enhancing contact interactions like the weak interaction. For example, atomic parity-violation effects, which measure the strength of the neutral weak interaction, scale with Z^2N, with additional relativistic enhancements of the electron's wavefunction and momentum at the nucleus (N is the number of neutrons). Effects in atoms from potential time-reversal violating electric dipole moments are predicted to show similar enhancements, including enhancements from nuclear structure effects like octupole deformation. Many of the most promising enhancements at high Z are in elements where all isotopes are radioactive, inherently limiting the number of atoms that can be produced. The traps enable the possibility of tests in such isotopes, utilizing precision techniques developed recently in the atomic physics community.

The weak couplings are also universal in the sense that the quark couplings are given in terms of the lepton couplings. The weak coupling between nucleons is not fully understood, even phenomenologically [7]. Measurement of the nuclear anapole moment in traps could resolve a present discrepancy between the anapole moments of cesium and thallium and low-energy nuclear physics results.

1.2. How a MOT works

It is useful to first describe the workhorse trap in this field, the magneto-optical trap (MOT), sketched in figure 1. A MOT can be treated as a damped harmonic oscillator [8]. The damping is provided by laser light from six directions tuned a few linewidths lower than the frequency of an atomic resonance ('to the red') . Atoms moving in any direction see light opposing their motion Doppler shifted closer to resonance, and preferentially absorb that light and slow down. This works naturally in three dimensions to cool the atoms.

To have a linear restoring force, one must evade the 'optical Earnshaw theorem'. Consider Poynting's theorem for the divergence of the momentum $\vec{S}$ carried by a plane wave

$$\vec{\nabla} \cdot \vec{S} = \frac{c}{4\pi} \vec{\nabla} \cdot (\vec{E} \mathrm{x} \vec{B}) = -\vec{J} \cdot \vec{E} - \frac{\partial u}{\partial t}. \tag{1}$$

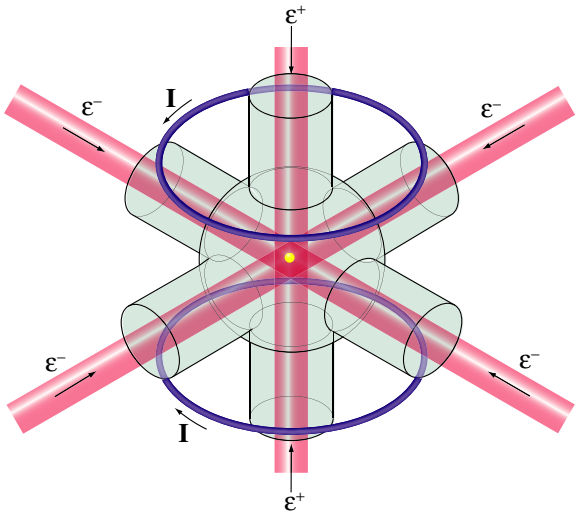

Figure 1. Schematic of a three-dimensional magneto-optical trap (MOT). Beams from 6 directions tuned lower in frequency than atomic resonance slow the atoms. Coils with opposing currents produce a weak magnetic field that is linear in all three dimensions, producing a linear restoring force by increasing the probability of absorption from whichever beam pushes toward the center (see figure 2).

This vanishes in a source-free region, when time is averaged over a period of the light wave. When the divergence of the Poynting vector is zero, there cannot be a three-dimensional trap for point particles from continuous plane waves of light [9, 10] (by analogy with the Earnshaw theorem for charged particles in electrostatic fields). The loopholes in this theorem are found directly in the conditions listed: either internal degrees of freedom of the atom are used to make them not pointlike, or time dependence of the light can be harnessed.

Ashkin and Gordon, the authors of [9], immediately implemented the use of the 'dipole force' to manipulate the internal degrees of freedom of the non-pointlike atoms [11]. If a laser beam is tuned very far-off atomic resonance, almost no photons are absorbed. Instead, the electric field $\vec{E}_{\text{laser}}$ of the laser light polarizes the charge of atoms by the AC Stark shift. The resulting induced electric dipole $\vec{d}$ then couples to $\vec{E}_{\text{laser}}$, producing a potential energy change of the atom $-\vec{d} \cdot \vec{E}_{\text{laser}}$. One version of this trap is simply a laser beam focused to a diffraction-limited spot, which produces a spatial gradient of $-\vec{d} \cdot \vec{E}_{\text{laser}}$ in all three dimensions. This creates a conservative trap without damping, with typical well depths of order 10^{-3} Kelvin. Such dipole force traps are widely used [12]. Since they are conservative, they must always be loaded using other dissipative techniques.

There are also time-dependent forces from pulsed lasers that have been shown to provide strong forces by alternately exciting and stimulating photon absorption [13]. Similar 'bichromatic' forces where the time dependence effectively comes from beats between different light frequencies have also been harnessed [14, 15].

Dalibard is credited with the most successful idea to manipulate the internal structure of the atoms to preferentially absorb the beam directing atoms to the center, the MOT [16], which is shown schematically in figure 1. The linear part of the restoring force is provided by a weak magnetic quadrupole field with gradient $\sim$10 G cm^{-1} produced by anti-Helmholtz coils. This B field changes sign at the origin, changing the sign of the Zeeman splitting and

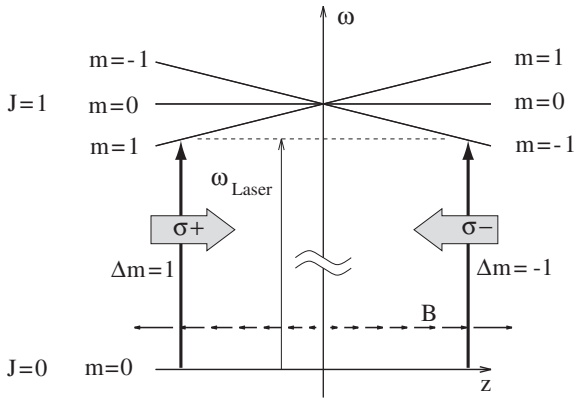

Figure 2. Simple one-dimensional MOT model for an atom with a $J = 0$ ground state and $J = 1$ excited state. In the center the magnetic field is zero and the laser has a red detuning of about one to two natural linewidths to provide Doppler cooling. The linear field gradient introduces a Zeeman splitting which together with the handedness of the counter-propagating beams creates the position-dependent force. The MOT quadrupole field produces such linearly changing B fields along each axis, $\vec{B} \approx B_0(2\vec{z} - \vec{x} - \vec{y})$. In the trapping literature the light polarization is described by the projection of the photons' angular momentum onto a fixed quantization axis (here the z-axis), leading to the shown $\sigma^+ - \sigma^-$ configuration for the MOT; the counter-propagating beams therefore have the same handedness ϵ^+; in addition, the beams in the x–y plane have the same handedness ϵ^- opposite to that of the z beams (running through the coils in figure 1). Adapted from [8].

therefore the probability of absorbing circularly polarized light with opposite handedness in the opposing beams (see figure 2). Coupled with the damping from the red detuning described above, this makes a dissipative trap that cools and confines atoms. The depth can be on order 1 K. The ability of the MOT to cool atoms makes it a typical first trap which then often feeds conservative traps.

The MOT's magnetostatic potential is more than an order of magnitude smaller than what is typically used to confine atoms directly in magnetostatic traps [17]. The magnetic field of the MOT is mainly being used to induce the atoms to absorb one beam or the other. The result is generally an overdamped harmonic oscillator, with a cloud of atoms $\sim$1 mm in diameter collected at the origin. Because of the different light polarizations in the six beams, a normal MOT will have atomic and nuclear-spin polarization close to zero, though modified geometries have been used to deliberately spin-polarize atoms [18]. Because of the near-resonant laser light, MOTs are inherently highly isotope and isomer selective. The mean lifetime of atoms in the MOT is $\sim$1 s at a vacuum of 10^{-8} Torr, limited by the average collision cross-section with background gas, as the momentum transfer in most collisions is more than adequate to eject the trapped atom. A more complete treatment of laser forces on atoms can be found in [19].

1.3. MOT-based tests of the weak interaction

From the experimental properties of the MOT, one can immediately see several broad classes of experiments that MOTs can assist.

The low-energy ($\sim$100 eV) nuclear recoils from β decay freely escape the MOT—they have transmuted to another element so the laser light no longer matters, and the B field is very small. Using an apparatus similar to figure 3, the recoils can be accelerated in a known electric

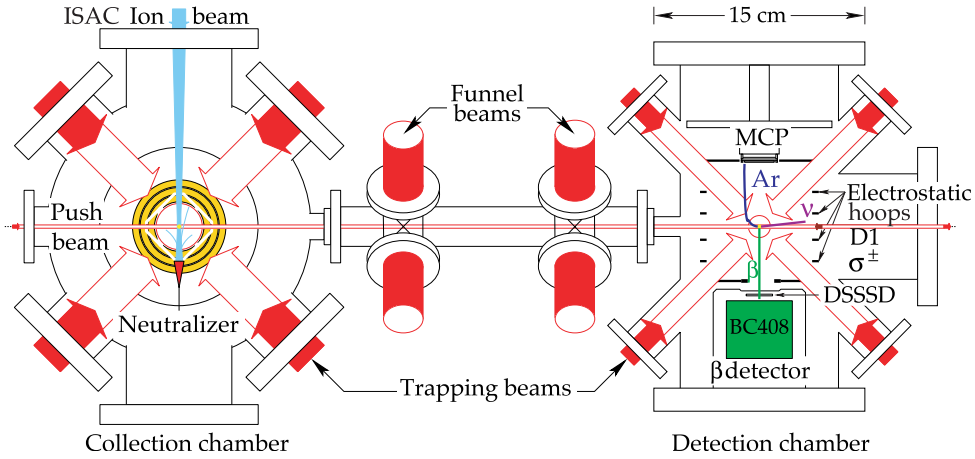

Figure 3. Prototypical TRIUMF Neutral Atom Trap 2-MOT apparatus. A vapor-cell MOT traps radioactives with 0.1% efficiency, and then the atoms are transferred with high efficiency [21] to a second trap with detectors. A uniform electric field collects ion recoils to a microchannel plate, where their position and time-of-flight (TOF) with respect to the β^+ is measured. An additional beam ('D1 $\sigma^{\pm}$') can spin polarize the atoms by optical pumping when the MOT is off.

field to a microchannel plate (MCP). Their time and position of arrival at the MCP, along with their known initial position in the trap cloud (which has size ∼1 mm), allows their momentum to be deduced. Together with measurement of the β momentum by more established detection techniques, this allows the reconstruction of the ν momentum in a much more direct fashion than possible previously. (Measurement of the β energy is difficult, but there are kinematic regimes—recoil momenta less than Q/c, where Q is the maximum β kinetic energy—for which the neutrino momentum is uniquely defined from the other kinematic observables [20]; see section 2.2.1.) Therefore, the angular distribution of ν's with respect to the β direction, the β–ν angular correlation, can be measured.

A variety of methods exist to polarize laser-cooled neutral atoms and to accurately measure their polarization, and some will be described in section 2.4. Knowledge of the polarization of the decaying species is a limiting systematic error in many neutron β decay and μ decay experiments. For most experimental tests of maximal parity violation, the polarization must be known with error less than 0.1%.

The cold, confined atom cloud also provides a bright source for Doppler-free precision spectroscopy of high-Z radioactive atoms. On the order of 10^7 photons s^{-1} are emitted into 4π for a saturated electric dipole transition. Forbidden transitions that move atoms from one state to another can then be probed efficiently by laser probes exciting allowed transitions. The atoms can also be interrogated repeatedly by strong laser, microwave and electric fields in well-controlled environments. We will see several examples of these powerful techniques below.

1.4. What elements can be trapped?

Tens of thousands of photons must be absorbed to slow atoms from room temperature, so until recently it was assumed that neutral atoms must have reasonably strong cycling transitions to be trapped (for a cycling or closed transition, spontaneous decay immediately returns the atom back to the state from which it was excited by the laser, leading to continuous

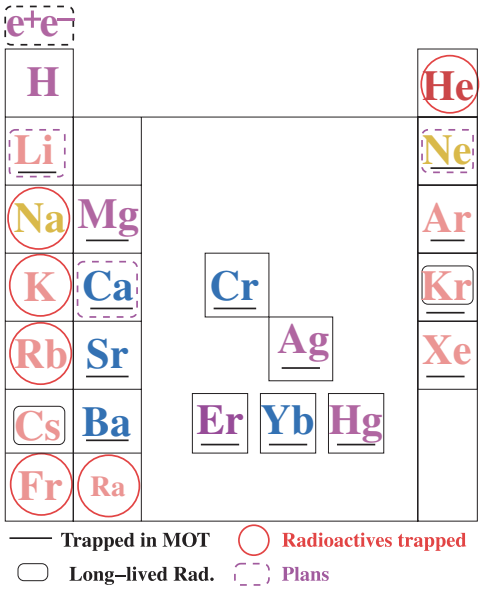

Figure 4. The periodic table of elements that have been laser cooled and/or trapped. The approximate laser wavelength is color-coded (online). Additionally, laser-cooled atoms include hydrogen, aluminum and iron. Based on a figure by GD Sprouse.

re-excitation and strong fluorescence). It is best if the excited state atomic angular momentum $J_{\text{excited}} = J_{\text{ground}} + 1$, so that all ground state sublevels can be excited by circularly polarized light. Figure 4 shows elements that have been laser-cooled and/or trapped.

Alkali atoms have a single electron outside a closed noble gas core, which makes them ideal cases. Typically the $s_{1/2} \rightarrow p_{3/2}$ transition is used. If the nuclear spin $I \neq 0$, then hyperfine splitting produces two ground states with total angular momentum $F = I \pm \frac{1}{2}$. The transition $F = I + \frac{1}{2} \rightarrow F = I + \frac{3}{2}$ is then cycling, since decays from $F = I + \frac{3}{2}$ to $F = I - \frac{1}{2}$ do not proceed by allowed electric dipole transitions. Most of the light is applied just to the red of this 'trapping' transition. Because of weak off-resonant excitation to $F = I + \frac{1}{2}$ excited states, eventually atoms would accumulate in the $F = I - \frac{1}{2}$ ground state, so additional, typically much weaker, 'repumping' light is also applied nearly resonant with a transition from that state, feeding atoms back into the right ground state. Radioactive isotopes of most alkali elements (Na, K, Rb, Cs, Fr) have been trapped.

Alkaline earths can also be trapped with shorter-wavelength E1 transitions if additional lasers are used to remove atoms from metastable states. Barium, which requires complex repumping schemes, has recently been trapped [22]. Radium atoms have states with potential enhancements of time-reversal violating electric dipole moment (EDM) and anapole moment effects [23]. Researchers at Argonne National Lab have succeeded in trapping radium, using a mixed transition at 714 nm with ∼10% of an allowed E1 strength [24, 25].

Typically, the first four excited states of a noble gas will have two metastable states from which there are single-electron cycling transitions accessible with lasers. Therefore, they can be trapped if the metastable states are first populated by some other method, e.g. by using a Penning discharge. For example, radioactive isotopes of He and Kr have been trapped. ^{6}He and ^{8}He have been trapped by the Argonne group, and their charge radii determined via optical

isotope shift measurements [26, 27]. Trace analysis has been done on long-lived Kr isotopes by the same group [28].

Other elements can be trapped if sufficient effort is given to the lasers. Laser-cooling transitions in a number of unusual species were proposed by Shimizu [29]. Adams and Riis [30] review the successfully trapped elements. Since that review, stable isotopes of Ag [31], Cr [32], Yb [33] and Hg [34] have been trapped in a MOT for studies of clock standards, Fermi degenerate gases and Bose condensates, and EDM searches. These elements still have relatively simple electronic structures.

In contrast, the complex rare earth atom erbium has now been laser-cooled and trapped [35, 36]. Erbium has an optical transition possibly useful for a time standard. A single-frequency laser was used. There are more than 50 states between the excited state in the main laser transition and the ground state. The large atomic angular momentum ($J = 7$ ground state) makes transitions to most of these states weak, minimizing the loss of population to long-lived low-J metastable states. The high J also produces a large atomic magnetic moment, so the weak MOT quadrupole field is thought to help contain the atoms during the time they are in metastable states. This opens the door to trap other complex systems with large atomic angular momentum, for whatever specific cases prove to be useful.

A rather more exotic possibility would be the trapping of orthopositronium, for which work has been done at Tokyo Metropolitan University [37]. The goal of this would be a Bose–Einstein condensate to produce coherent annihilation γ-ray emission [38].

1.4.1. Loading the shallow MOT for alkalis. The MOT depth is on order one Kelvin. Each group trapping radioactive isotopes has invested large efforts to learn to load a MOT efficiently in geometries appropriate for their particular experiments. The creation of the radioactives inherently involves a production target where nuclear reactions produce too much background for any type of experiment, so the isotopes must be transported away from this region. The final vacuum, desired at the 10^{-10} Torr level, also involves challenges. The first two groups which trapped radioactives solved these problems in quite different ways, and most efforts since then have made improvements along the same lines.

In the initial Stony Brook work trapping ^{79}Rb [39], a heavy ion beam induced fusion reactions in a foil that was a combination target and surface ionizer. The products were transported as a low-energy ion beam [40]. The ions were implanted in a surface with a low work function (yttrium) to keep the evolving atoms neutral. The atoms were collimated into an atomic beam feeding a vapor-cell lined with silicone polymer coatings to which the alkali atoms do not stick [41, 42]. The vapor cell confined the atoms for many passes through the beams and many chances to be trapped, after re-thermalization upon contact with the walls replenished the low-velocity tail of the Maxwell–Boltzmann velocity distribution [43].

The short-lived isotope ^{21}Na trapped at Berkeley was produced as a collimated atomic beam from a hot magnesium oxide production target. The atoms were slowed longitudinally by an unopposed laser beam as they traversed inside a tapered solenoid utilizing the Zeeman effect to keep the atoms in resonance (a 'Zeeman slower') before they entered the trap [44].

We show the TRIUMF Neutral Atom Trap (TRINAT) system as a typical example for the loading and preparation process [45] (figure 3). A mass separated 30 keV ion beam from TRIUMF's ISAC facility [46] is stopped in a 900 °C Zr foil, adapting a geometry pioneered at Los Alamos [47] to use a conical neutralizer to minimize implantation depth. Only atoms moving at less than about 5–10% of room temperature velocities can be trapped. Typical efficiencies for trapping atoms in a vapor cell are 0.1–1%. To avoid the large radioactive background from untrapped atoms, both in the untrapped vapor and on the walls, 75% of the cooled atoms are transferred in TRINAT to a second MOT where the experiment takes

place. The transfer time is 25 ms. Details of the transfer process are in [21]. For atomic physics experiments on stable species, the two-MOT arrangement is also common to improve the vacuum, avoid the small backgrounds from the Doppler-broadened vapor, and allow specialized apparatus surrounding the second MOT.

Vapor-cell MOT efficiencies of 50% have been reported in stable species [48], where efficiency is defined as the percentage of incoming atoms that are loaded into the trap. Efficiencies for radioactive species have not exceeded 5×10^{-3}, reported by the Los Alamos group [47, 49]. Possible ways to increase the capture velocity that have been used on stable species include frequency combs farther to the red [50], white light slowing [51], and light-assisted desorption [52]. The MOT relies on the emission process being front–back symmetric with respect to absorption, so it is limited by the spontaneous atomic decay rate, and it does not help to increase laser power beyond saturation. Stimulated forces, like the bichromatic forces mentioned above [15], have been demonstrated to slow stable Cs in one dimension from room temperature over a distance of 10 cm [14], and they have the promise of being limited only by the laser power applied (admittedly, for many atoms lasers have insufficient power to saturate the spontaneous forces.)

The traps are highly element, isotope and isomer selective. For example, at TRIUMF/ISAC the mass separated $A = 38$ ion beam has 20 times more of the ground state of the isotope ^{38}K (spin and parity $I^\pi = 3^+$, $t_{1/2} \sim 7$ minute) than the nuclear isomer ^{38m}K of interest ($I^\pi = 0^+ t_{1/2} \sim 1$ sec). The $I^\pi = 3^+$ nuclear ground state has an atomic ground state hyperfine splitting of 1.4 GHz, and these states straddle equally the location in atomic energy of the 0^+ isomer. The MOT works at frequencies from 5 to 50 MHz to the red of resonance, but more importantly, two frequencies are required to trap the hyperfine split 3^+ state. Hence, the one frequency applied to the MOT only traps the 0^+ nuclear isomer. No recoil-β coincidences were observed from the decay of the 3^+ state [45].

2. Atom traps for decay experiments

In this section we describe the use of atom traps for nuclear beta decay, both with spin polarization and without. We also describe missing-momentum searches for sterile neutrinos in β decay and electron capture, along with other exotic particle searches in isomer decay.

We expand informally upon our introduction to β decay in section 1.1. For a more complete and technical review, see [53]. At these low momentum transfers, β^- decay in the Standard Model or any extension based on exchange of very massive bosons reduces to a sum of 4-fermion contact interactions [54]

$$H_{\rm int} = \sum_X (\bar{\psi}_p O_X \psi_n)(C_X \bar{\psi}_e O_X \psi_\nu + C'_X \bar{\psi}_e O_X \gamma_5 \psi_\nu), \tag{2}$$

where O_X denotes operators with the five different possible Lorentz transformation properties X—vector (V), axial vector (A), tensor (T), scalar (S), and pseudoscalar (P)—and implicitly includes all necessary contracted relativistic 4-indices. This interaction then is invariant under Lorentz transformations.

The combinations of C_X and C'_X produce projection operators $1 \pm \gamma_5$ which project out either left or right-handed neutrinos. In the Standard Model, the interaction between quarks and leptons is 'V–A', so if we had written the interaction between quarks and leptons, then $C_V = C'_V$ and $C_A = -C'_A$, the combination given by exchange of the spin-1 W boson. Then only left-handed neutrinos are emitted.

The absolute value of C_A departs from unity as QCD combines quarks into nucleons, but the interaction still produces only left-handed neutrinos. Similarly, though all other constants

besides V and A would be zero in the SM quark–lepton interaction, similar terms become in principle allowed again in the nucleon–lepton interaction; these are termed 'induced (by QCD) currents'. Many of the induced currents would violate what is called G-parity, which reduces to charge symmetry in the first generation of particles, and were therefore termed 'second-class currents' by Weinberg [55] and removed from the SM. Thus the scalar constants C_S and C'_S are still zero in the SM, as they are second-class currents, and they also violate the conserved vector current (CVC) hypothesis. In fact fundamental quark–lepton scalars cannot be distinguished experimentally from induced scalar interactions [56]. Greater care must be taken to distinguish experimentally between tensor non-SM quark–lepton interactions and allowed induced tensor currents. In isobaric analog decays (like that of the neutron, or ^{21}Na and ^{37}K below) the extra induced tensor-order interactions are either given by CVC in terms of the electromagnetic moments, or vanish because they are second-class currents [57].

The general expression for the nuclear beta-decay rate W in terms of the angular correlations and distributions of the leptons, including the possible spin-polarization of the nucleus, is given (using lepton momenta $\vec{p}$ and energy E and nuclear-spin polarization and unit direction $\vec{I}$ and $\hat{i}$) by [58]

$$W\,\mathrm{d}E_e\,\mathrm{d}\Omega_e\,\mathrm{d}\Omega_\nu = \frac{F(\pm Z, E_e)}{(2\pi)^5} p_e E_e (E_0 - E_e)^2\,\mathrm{d}E_e\,\mathrm{d}\Omega_e\,\mathrm{d}\Omega_\nu \frac{1}{2}\xi \times \left[1 + a\frac{\vec{p}_e\cdot\vec{p}_\nu}{E_e E_\nu} + b\frac{m}{E_e} + c\left(\frac{1}{3}\frac{\vec{p}_e\cdot\vec{p}_\nu}{E_e E_\nu} - \frac{\vec{p}_e\cdot\hat{i}}{E_e E_\nu}\right)\left(\frac{I(I+1) - 3\langle(\vec{I}\cdot\hat{i})^2\rangle}{I(2I-1)}\right) + \frac{\langle\vec{I}\rangle}{I}\cdot\left(A_\beta\frac{\vec{p}_e}{E_e} + B_\nu\frac{\vec{p}_\nu}{E_\nu} + D\frac{\vec{p}_e\times\vec{p}_\nu}{E_e E_\nu}\right)\right], \tag{3}$$

where F is the Fermi function. We will discuss below trap measurements of the β–ν correlation coefficient a, the β asymmetry with respect to spin A_β, the ν asymmetry with respect to spin B_ν, and the time-reversal violating correlation coefficient D. The second-rank tensor alignment term with coefficient c occurs for nuclear spin $I \geqslant 1$. Explicit expressions for these experimental observables as a function of the C_X constants were worked out in [58], and can be found rewritten in explicitly chiral notation in the review of [53]. Rather than rewrite these expressions, we discuss qualitative features here. We ignore here observables that measure the spin-polarization of the leptons, as these have not been pursued as yet with traps.

In equation (3) we can see that the correlations are all normalized by the change in decay strength due to the term b. The decay rate and angular distributions are given by the absolute square of the matrix elements of H_{int}. That produces cross terms between new interactions and the SM interactions that are therefore linear in the small new coupling coefficients. Such 'Fierz interference terms', collected together as b in equation (3), always produce left-handed neutrinos, just as the SM does. So searches confined to them already assume the complete chirality and good time-reversal symmetry of the SM. This is a natural thing to do in many theories, and many limits from particle physics in the literature simply assume this chirality without qualification.

Terms are also produced that are squares of the new interactions. We will give simple arguments below why the beta–neutrino correlation is sensitive to these. These terms are more general in the sense that they are insensitive to the chirality and time-reversal symmetry properties of the new interactions.

To take an example of an explicit model, one possible source of non-Standard model scalar and tensor interactions is supersymmetry. Profumo *et al* [59] have shown in a wide variety of SUSY models that left–right mixing between supersymmetric partners of the first-generation

fermions can generate terms as large as 0.001 in the Fierz interference scalar–vector and tensor–axial vector terms. This left–right sfermion mixing is difficult to constrain in particle physics searches. It is a goal for many of the correlation experiments discussed below to reach such sensitivity.

We also note here one possibly confusing fact: a spin-0 leptoquark (i.e. a particle explicitly changing leptons into quarks) can generate both 4-fermion scalar and tensor effective interactions [60]. Consequently, a fundamental interaction producing a 4-fermion effective tensor interaction does not imply some very exotic spin-2 particle.

2.1. Recoil momentum from traps: Beta–neutrino correlations, motivation

Historically, the β–ν angular correlation (the a term in equation (3)) has provided some of the best evidence that the effective contact interaction was primarily vector and axial vector, which in modern theories is due to exchange of the spin-1 bosons.

Adelberger pointed out the utility of such measurements in pure Fermi decay to constrain scalar interactions [62]. One can make a simple helicity argument to show that $a = 1$ for these decays. The leptons are produced with opposite helicity in the Standard Model interactions. For $I^\pi = 0^+ \rightarrow 0^+$ decays, where the leptons must carry off no angular momentum, they cannot be emitted back-to-back. Thus these experiments are insensitive to the absolute chirality of the couplings, and only depend on the relative helicity of the two leptons. They are sensitive to the sums of absolute squares of the scalar or tensor interactions in equation (2). Although one is measuring the square of small terms, this is a large advantage when looking for wrong-chirality interactions that do not interfere with the Standard Model's one-sign chirality.

The Fierz interference terms also modify the decay rate and therefore the normalization of the angular distribution. The β–ν correlation also has linear sensitivity to some of the new physics.

2.2. Beta–neutrino correlations: experiment

2.2.1. β–ν correlation of ^{38m}K. TRIUMF's Neutral Atom Trap Group (TRINAT) has published its β–ν correlation result for ^{38m}K, a pure Fermi decay sensitive to scalar interactions [45]. The result for the angular distribution coefficient $a = 0.9981 \pm 0.0030$ (statistical) ± 0.0037 (systematic) is in agreement with the Standard Model value of unity. It has somewhat greater accuracy than the Seattle/Notre Dame/ISOLDE work in β-delayed proton decay of ^{32}Ar [63], which set the previous best general limits on scalars coupling to the first generation of particles. (The ^{32}Ar work, re-evaluated after re-measurement of the decay energy, gives $a = 0.9980 \pm 0.0051$ (statistical) with systematic error to be determined [64].) The TRINAT work was done with two thousand atoms trapped at a time, at densities less than 0.5% of those in the Berkeley work, avoiding the possibility of trap density distortions (see below).

The nuclear detection is done using the right-hand MOT apparatus of figure 3, as discussed in section 1.3. A scatter plot of 500 000 β^+-recoil coincidence events from the decay of ^{38m}K is shown in figure 5. The solid lines are the kinematic loci that would result from back-to-back pointlike detectors. If the two leptons are emitted in a similar direction, the recoil momentum is very similar (the β's are relativistic so the energy sharing between leptons matters little), producing large numbers of events with similar time-of-flight (TOF) for each charge state. When the leptons are emitted close to back-to-back, the recoil momenta are much smaller, producing the arcs at longer TOF. One can immediately see qualitatively that the leptons are rarely emitted back-to-back. These spectra are binned in TOF and β energy, and a fit to a detailed Monte Carlo simulation is used to extract the quantitative angular distribution [45].

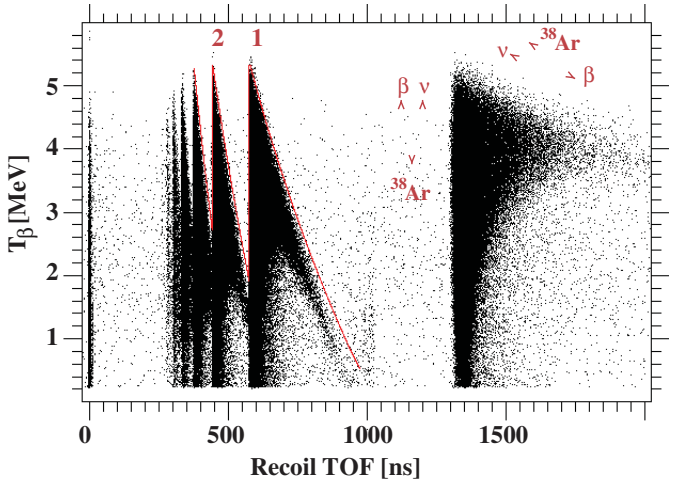

Figure 5. Scatter plot of ^{38m}K β-recoil correlation data. The recoils are produced in several charge states ranging from neutral atoms to ions of charge 1–6, which are separated by their time-of-flight (TOF) in the uniform electric field of figure 3. The arrows denote lepton and recoil momenta (see the text).

Background events can also be rejected if they are not kinematically allowed. At 1025 ns in TOF in figure 5, there are events at part per thousand probability at low measured β^+ energy. These originate from $\beta's$ that are emitted toward the MCP—sending recoils away from the ion micro-channel plate (MCP) to be collected by the electric field at later times—then scatter off material and into the β^+ detector.

The energy response of the β detector is critical in this type of β-recoil coincidence measurement. TRINAT can determine detector response functions *in situ* from the actual data. This is typically done in high-energy experiments but never before for low-energy β decay. Consider, for example, a TOF cut of 750–850 ns in figure 5. These ions of charge state +1 come from events with a narrow range of β^+ kinetic energy centered around 2.2 MeV. Events with lower detected β^+ energy are produced by the imperfect β^+ energy determination of the β^+ detector in figure 3. The β^+ energy can be more precisely reconstructed by including the β^+ direction information from the position-sensitive ΔE detector. Figure 6 shows the energy response of the β detector to the monoenergetic β's obtained this way.

Limits on scalar couplings. The limits on scalar interactions from two sources are shown in figure 7. There are tight constraints on the scalar–vector Fierz interference term from the superallowed ft values as a function of energy release [61], because the Fierz term depends on the β energy (equation (3)). The β–ν correlation sets more general constraints on scalars that couple to either left or right-handed neutrinos [63]. The β–ν correlation results from ^{32}Ar have the same centroid as ^{38m}K with somewhat larger total error [64], and when that final error is decided the allowed area will decrease somewhat. Powerful but model-dependent constraints from $\pi \rightarrow e\nu$ decay are considered in [65]. A scalar interaction coupling to right-handed neutrinos produces a mass for the SM neutrino, and order-of-magnitude estimates for this effect were done in [66].

2.2.2. β–ν correlation of ^{21}Na. The laser-trapping group of Lawrence Berkeley Lab had earlier published the first β–ν correlation using an atom trap [67]. Their abstract quotes the

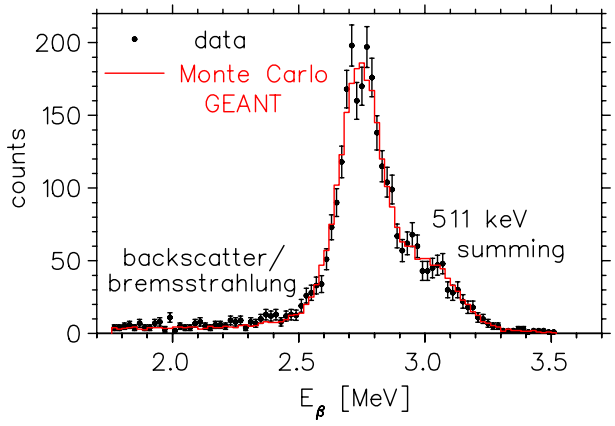

Figure 6. Energy response of the β^+ detector plastic scintillator of figure 3 to 'monoenergetic' β^+'s (with total energy from 2.7–2.8 MeV) as determined from the β-recoil angle and recoil momentum (see the text). Events where less energy is deposited in the detector are produced by backscattering out of the detector and by emission of bremsstrahlung γ-rays. Some annihilation 511 keV γ-rays Compton scatter in the scintillator, producing the higher-energy knee. The width of the main peak is dominated by the energy resolution of the plastic scintillator.

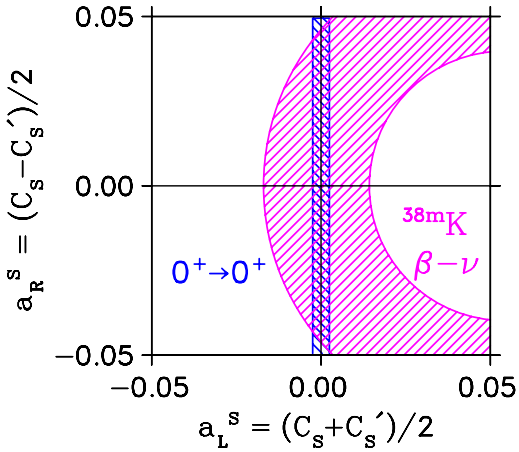

Figure 7. Constraints at 90% CL on scalar interactions, from 0^+ to 0^+ ft values [61] (rectangle) and from the TRINAT ^{38m}K β–ν correlation [45] (concentric circles).

result $a = 0.5243 \pm 0.0091$ for ^{21}Na, which has a Standard Model prediction of 0.558. A Gamow–Teller branch to an excited state was subsequently remeasured by several groups, although to explain the full deviation the branch would have had to be 7% rather than the compiled value of $5.0 \pm 0.13\%$, and the new more precise measurements produced only slight changes from the compiled value [68].

The Berkeley group presented evidence for a dependence of a on the density of atoms trapped for more than 10^5 atoms trapped. If an extrapolation to zero density was done, the value for a was brought into agreement with the Standard Model, $a = 0.551 \pm 0.0013 \pm 0.006$ [67]. They have since definitively characterized the effect (see the following section 2.2.3).

2.2.3. Trap-produced perturbations. Since the atoms trapped are not ideal point particles, it is important to note some of the complications produced by atomic physics and trap effects.

Formation of ultracold molecules. Deliberate formation of ultracold molecules has produced a large number of precise experiments in stable species. Electric dipole transition matrix elements between p-state and s-state atoms can be deduced by the frequency dependence of photoassisted collisions [69]. The ultracold molecules themselves are very interesting to chemists and to proposed precision measurements including anapole moments, searches for permanent electric dipole moments, and quantum computation [70]. Unfortunately, they also produce malevolent effects in beta–neutrino correlations.

The Berkeley group suggested a possible mechanism for a density-dependent effect in their measurement of the β–ν correlation. Distortions of the recoil momentum are produced when the decay originates from a molecular dimer magnetostatically confined within the MOT's weak quadrupole B field. They have observed the molecular dimers, and inhibited their formation by using a dark spot MOT.

They also developed a high-statistics data technique, measuring the shakeoff electrons with high efficiency in coincidence with the recoils. The resulting TOF spectrum is almost equivalent to a momentum spectrum of the recoils. Sensitivity to a is inherently lower than in the β-recoil coincidence, but the overwhelmingly higher count rates produce a smaller statistical error on a. After accounting for the measured dependence of the measured a on trap density, the result is $a = 0.5502 \pm 0.0060$ [71], in agreement with the Standard Model prediction 0.553 ± 0.002.

It is important to realize that the frequencies and strengths of the photoassociation resonances are a strong function of fine and hyperfine structure, and their effects on the determination of a must be determined in future experiments on an isotope-by-isotope basis.

Doppler shifts are small. The remaining Doppler shifts after laser cooling are negligible for nuclear β–ν angular correlation decay. Possible experiments in electron capture producing recoils with kinetic energies ∼eV will require sub-Doppler cooling (see section 2.3.1 below), which generally comes for free in careful MOT experiments [72].

2.2.4. Atomic charge state dependence on recoil momentum. Work at Berkeley and TRIUMF has confronted an additional systematic error common to most other recoil momentum measurements, the possibility that the final atomic charge state depends on recoil momentum [73]. If the charge state of the atom depends on recoil or beta momentum, the deduced angular correlations are perturbed. This effect is a potentially important correction to many atom and ion trap β–ν experiments, so we sketch some details here.

Momentum-dependent shakeoff was first postulated, modeled, and measured in ^{6}He β^- decay work at Oak Ridge [74]. Atomic electrons in the daughter can be treated as suddenly moving with the recoil velocity. A plane wave expansion of the resulting sudden approximation matrix element produces an effect proportional to the square of the recoil velocity. Hence, the sudden approximation to lowest order produces a distortion of the recoil energy spectrum of the form $(1 + sE_{\rm rec}/E_{\rm max})$, where $E_{\rm rec}$ is the recoil kinetic energy, and $E_{\rm max}$ is the maximum value of the recoil kinetic energy. A simple estimate by the Berkeley group relates the size of the parameter s to atomic dipole oscillator strengths, and suggests that it could be larger in β^+ decay [73] because of the difference in atomic binding energies.

In the absence of detailed calculations of the momentum-dependent shakeoff, it can be constrained by fitting the above expression to experimental data and letting s float along with the coefficient a of the β–ν angular distribution, because they have different dependence on

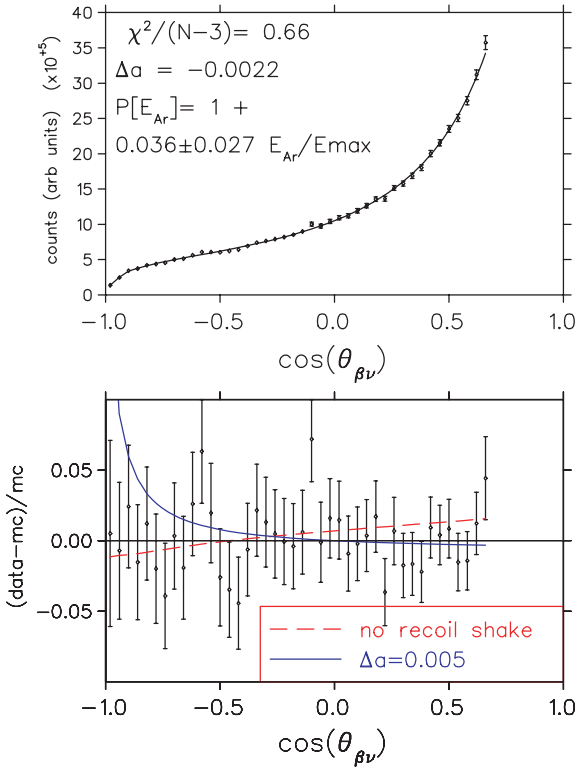

Figure 8. Top: the distribution of detected coincidence events as a function of the angle between β^+ and neutrino in ^{38m}K decay, as determined in the TRINAT apparatus. If all recoils were collected, this would be a straight line determining a (see equation (3)); here a Monte Carlo simulation includes the detector acceptance. Bottom: difference between experiment and model, normalized to model. The dependence of recoil electron shakeoff on the recoil momentum produces a different effect on the angular distribution than changes in a, so it can be simultaneously fit and shown to be small (see the text).

the kinematic variables. This was done in two separate analyses with the TRINAT data, using different combinations of kinematic variables, as discussed in [75, 45]. An example is shown in figure 8, where the change in the angular distribution due to s or to a is shown, with the result that s produces less than a 0.002 change in a [45]. The effect of s on the deduced value of a depends on the experimental geometry, the experimental observables, and on the value of a itself. In pure Fermi decays, the null in the β–ν angular distribution is helpful to tell the difference between the effects from s and changes in a. The effect of s will be more strongly correlated with a in experiments that solely consider the recoil energy spectrum.

2.2.5. Beta–neutrino correlation summary. Figure 9 summarizes the contribution of β–ν correlation measurements, including the trap work in ^{21}Na and ^{38m}K, to our knowledge of the Lorentz structure of the weak interaction. On the horizontal axis is plotted a variable showing the degree of Fermi versus Gamow–Teller strengths. The solid line shows the prediction of V and A interactions. Note that the relative sign between V and A is not determined, as the β–ν correlation is not sensitive to parity violation. The dashed line shows the prediction of a pure S,T theory. The history of this plot is quite interesting, as in the late 1950's and early

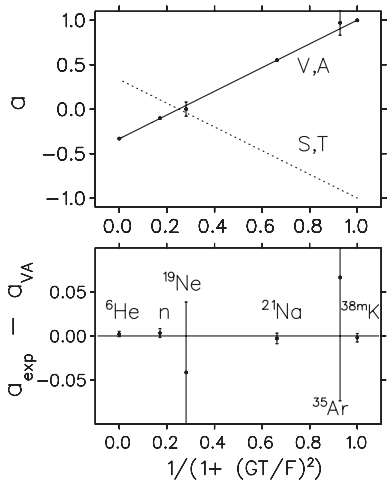

Figure 9. Present status of constraints on non-V,A interactions from measurements of the β–ν angular correlation coefficient a, updated from [76] (and as first plotted in [79]). The trap experiments in ^{21}Na [71] and ^{38m}K [45] are shown, along with previous ^{6}He [77], n [78], ^{19}Ne [79] and ^{35}Ar [79] measurements by other techniques. 'GT' and 'F' are the Gamow–Teller and Fermi matrix elements, so the x-axis variable is unity for pure Fermi decay and zero for Gamow–Teller decay. The two trap-based β–ν correlation results show the utility of constraints with large Fermi components.

1960's there were conflicting experimental results in the ^{6}He β–ν measurement. Respected yet colorful theorists favoring $V-A$ from their conserved vector current hypothesis suggested that those experiments which were in disagreement must be wrong [80]. The eventual accepted measurement of a in ^{6}He [77][3], together with the other measurements of figure 9, produces tight constraints in agreement with the interaction being purely V and A.

It is important to recognize that the nuclear structure corrections at this level are minimal and well under control. The pure Fermi case, ^{38m}K, is one of the well-characterized isobaric analog superallowed ft cases. The helicity argument to derive the β–ν correlation given above relies only on angular momentum conservation, and isospin mixing does not change the Standard Model prediction of $a = 1$. Second-order forbidden terms where the leptons carry off orbital angular momentum are suppressed to less than 10^{-6}. Radiative corrections produce real photons which, if undetected, perturb the momenta and produce a correction of $\approx$0.002 (corrected for in the Monte Carlo used in [45]). Recoil-order corrections enter at 3×10^{-4} [57] and are independent of nuclear structure. In an upgraded experiment, the TRIUMF group hopes to achieve 0.001 accuracy [81], so the smallness of the theory corrections is important.

We mentioned in section 2 that in mixed Gamow–Teller/Fermi transitions, higher-order corrections within the SM are given by CVC. The case of ^{6}He, while not such an isobaric analog decay, is also very favorable in terms of nuclear structure, because the higher-order corrections in β decay theory are either known or small. The recoil-order weak magnetism can be related to experimentally known M1 γ-ray decay by the CVC hypothesis, and although the first-class induced current d depends on nuclear structure, d is very small in this case because of accidentally favorable structure of the $A = 6$ nuclei [82]. The Paul trap measurement

[3] Which is a reanalysis including radiative corrections of second part of reference [77].

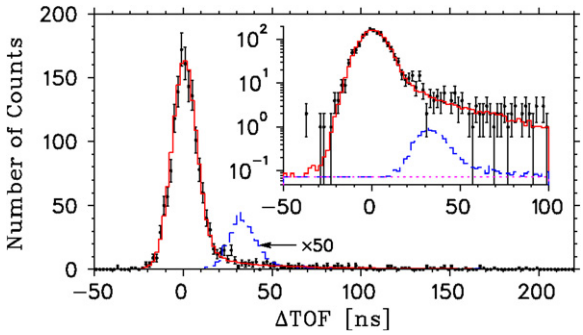

Figure 10. Search in ^{38m}K decay for a massive sterile neutrino having admixture with the electron neutrino. The experimental TOF spectrum is referenced to a simulation of recoils due to a zero-mass ν. A simulated 1 MeV ν (with admixture 50x larger than the experimental limit) makes the peak shown at delayed TOF, because it has lower momentum [83].

mentioned in the introduction is in ^{6}He [3], and the Argonne group is considering a β–ν correlation experiment in ^{6}He using a dipole force trap [84].

2.3. Recoil momenta from shakeoff electron coincidences

The Berkeley group's technique of using the atomic shakeoff electrons as a time-of-flight trigger [85] has other possible experimental applications.

There have been a number of estimates of the shakeoff electron kinetic energies, which are thought to be approximately twice their atomic binding energy. They can therefore be collected in the same electric field that collects the daughter ions into an MCP, and efficiencies of ∼50% can be attained. This enables a variety of high-statistics experiments. Experiments involving polarized nuclei are outlined in section 2.4. Here we describe searches for exotic particles in the recoil momentum spectrum.

2.3.1. Sterile neutrino admixtures. First we show the limitations of 3-body decays in missing mass searches.

TRINAT, using the neutral recoils from ^{38m}K decay (see figure 5), searched for admixtures of 0.7–3.5 MeV ν's with the electron ν [85]. The results are listed by the Particle Data Group [86]. The existence of such ν's could alter astrophysical observables [87][88], and they can be produced in models with extra dimensions [89]. The kinematic coincidences effectively reduce the 3-body kinematics to 2-body, and allow a search for peaks in a TOF spectrum instead of the more conventional search for kinks in continuous β spectra [90]. The admixture upper limits are as small as 4×10^{-3}, and are the most stringent for ν's (as opposed to $\bar{\nu}$'s) in this mass range, although there are stronger indirect limits from other experiments. Typical results are shown in figure 10.

The 3-body reconstruction is marred by the β detector energy response tail seen in figure 8, producing the smooth background seen in figure 10. Though this technique is an improvement over searching for kinks in β spectra, the sensitivity is limited by statistical fluctuations in the background and improves only with the square root of the counting time.

Two-body electron capture decay could provide a much cleaner method, and has the promise of improving existing limits by orders of magnitude. First we consider a simpler experiment in decay of nuclear isomers.

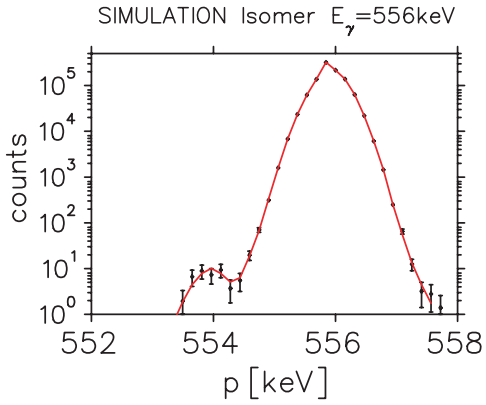

Figure 11. Simulation of the momentum spectrum from the decay of ^{86m}Rb. The smaller peak, from a hypothetical particle with mass 50 keV emitted with branch 4×10^{-5}, has lower momentum than the peak from γ-ray emission.

2.3.2. Searches for exotic particles in isomer decay. TRINAT has begun measurements of the momentum of monoenergetic recoils from isomer γ decay. This makes it possible to search for massive particles emitted by the nuclear transition instead of γ-rays. The recoiling nucleus would have lower momentum $p_x = \sqrt{E_\gamma^2 - m_x^2}$, producing a lower-momentum peak (see figure 11). This method does not rely on any information about the interaction of the particles in any detector, and is independent of the lifetime of the particle. Given produced yields from ISAC, sensitivity to decay branching ratios of $\sim 10^{-6}$ per day of counting for masses between 20 keV and 800 keV could be achieved using different Rb and Cs isotopes. Such an experiment would utilize high-momentum resolution spectrometer techniques developed for atomic physics experiments in the last decade [91], such as TOF drift spaces and electrostatic lenses to make momentum resolution less dependent on cloud size.

Angular momentum selection rules favor production of spin and parity $I^\pi = 0^-$ particles in transitions with magnetic multipolarity, and 0^+ particles in electric multipole transitions. In principle the isomers could also be spin polarized, and the measured angular distribution of the recoils would then determine the multipolarity of the emitted particle.

There are a—perhaps surprising—number of phenomenological motivations for such 'signature-based searches'. Although the mass range would seemingly have been explored long ago, potentially there is sensitivity to very small couplings that are otherwise difficult to constrain. These include light 0^+ particles associated with the annihilation radiation at the center of the Galaxy [92], 0^- particles with smaller couplings than the conventional axion that could still explain the strong CP problem [93], and 0^- particles from a different global U(1) symmetry that would explain the size of the μ parameter in SUSY [94]. Such an experiment is proceeding at TRIUMF in the decay of the 556 keV isomer in ^{86m}Rb. Sensitivity at the 10^{-6} level will need to be reached to be competitive with other, more conventional experiments in this field [95, 96].

2.3.3. Sterile neutrinos in electron capture decay. A goal is to extend these measurements to electron capture decay and search for sterile neutrinos with an admixture with the electron neutrino. A 1–10 keV mass ν_x with ν_e admixtures of $\sin^2(2\theta) \sim 10^{-8}$ would be a dark matter candidate [97, 98] and have other astrophysical implications [99, 100]. A theoretical

framework for such neutrinos also uses them to moderate inflation and produce the baryon asymmetry of the universe [101].

Possible experimental cases include ^{131}Cs, ^{82}Sr and ^{7}Be. A first-generation experiment in ^{131}Cs could reach statistical sensitivity to admixtures of $\sin^2(2\theta) \approx 10^{-5}$ for $m_\nu \approx 50$–300 keV. This would be two orders of magnitude better than present experiments, and would be useful to constrain scenarios with low post-inflation reheating temperatures that produce fewer sterile ν's [102].

Improving the mass resolution to ~10 keV would require the simultaneous detection and measurement of all Auger electrons, which carry off several percent of the momentum of the initial neutrino. Gating on X-ray transitions that select higher-lying atomic states with fewer Auger electrons could work, though that would push the energy resolution, efficiency and time resolution of X-ray detectors.

In more standard cosmological scenarios, there are stringent constraints on the admixtures of these neutrinos, as they tend to overclose the universe. These ν's have a two-body decay mode into $\nu_e + \gamma$, and direct searches for keV X-ray lines have set stringent constraints as well [103]. Nevertheless, theorists have suggested experiments in β-recoil coincidences in tritium decay that could reach this sensitivity [104].

2.3.4. Efficient magnetostatic loading techniques and tritium. An efficient loading technique which does not use laser cooling and can work on a very wide variety of neutral species has recently been demonstrated. Magnetostatic pulses switched with microsecond periods have been used to slow and trap Rb [105] and hydrogen [106] by different groups. The Rb atoms were then optically pumped to an atomic state with different g-factor to escape the magnetostatic trap and end up in a dipole force trap, a much better environment for precision spectroscopy. The proponents intend to trap tritium and measure the electron ν mass directly by β-recoil coincidences [105].

2.4. β-decay experiments with polarized nuclei

There are a number of possible correlations to measure if the nuclei are polarized (see equation (3)). Traps can provide high and well-quantified nuclear polarization. When combined with the detection of nuclear recoils, new and unique correlations can be measured.

2.4.1. Physics motivations for experiments with polarized nuclei. The Standard Model electroweak bosons couple only to left-handed neutrinos, and hence the current is termed V–A. Experiments with polarized nuclei in which the polarization can be known atomically can search for the presence of a right-handed ν. Much of the two-parameter space in the simplest 'manifest' left–right symmetric models has been excluded by proton–antiproton collider experiments and by superallowed ft values [61, 107]. Indirect limits from the K_L–K_S mass difference also strongly constrain left–right models, although these limits have some model dependence; e.g., reasonable simplifying assumptions must be made about the complicated Higgs sector in left–right models [60, 108].

However, in more complicated non-manifest left–right models, beta decay measurements with polarized nuclei are still competitive [53, 109]. For an example of a specific model, we mentioned above the semileptonic scalar and tensor interactions that can be produced in SUSY and produce observables at 0.001 level [59].

Second-class currents. The leptons and quarks come in weak isospin doublets, which provide cancellations necessary for the theory to be renormalizable [55]. When QCD dresses the

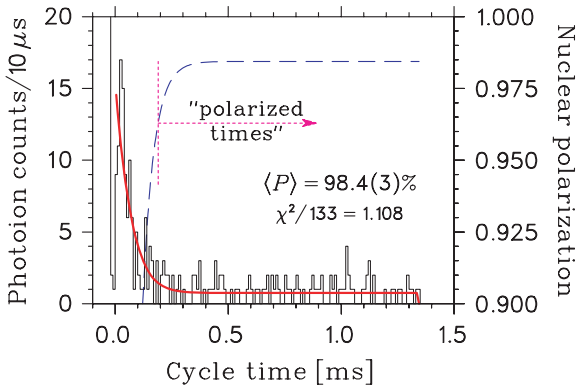

Figure 12. The near-vanishing of the fluorescence from the optical pumping of ^{37}K atoms, which both produces and non-destructively measures the polarization of the atoms and nuclei. The polarization (dashed line, right side axis) can be measured continuously for the same nuclei that decay [115] (see the text).

quarks into the non-Dirac particle nucleons, the isospin symmetry produces a number of constraints on the resulting possible currents. The absence of isospin-violating 'second-class' [110] currents can be tested in both polarized and unpolarized observables in isospin-mirror mixed Fermi/GT decays, like ^{21}Na and ^{37}K.

2.4.2. Experiments with polarized atoms in traps. The Berkeley group's publication of a also measured weak magnetism in agreement with the Standard Model [67], i.e. consistent with no second-class currents, although the value achieved is not yet competitive. Berkeley has measured precision hyperfine splittings in ^{21}Na using optical hyperfine pumping and microwave transitions [111]; these techniques are applicable to β-decay experiments with polarized nuclei.

After demonstrating polarization of ^{82}Rb ($t_{1/2} = 76$ s) in a magnetostatic TOP trap [112], the Los Alamos trapping group has since loaded a dipole force trap with 10^4 atoms of ^{82}Rb. They have observed an unusual spontaneous polarization phenomenon in this trap that has been observed before in dense gases, and this would be highly useful for β-decay experiments [113].

TRINAT has begun experiments with polarized ^{37}K by turning off the MOT and optically pumping [114] the expanding cloud. Circularly polarized laser light shines on the atoms (the 'D1' beam in figure 3). The atoms are excited to states with higher (or lower) angular momentum projection, then decay randomly back to different angular momentum projections. The state population undergoes a biased random walk, which eventually puts all the atoms into the ground state with highest (or lowest) angular momentum. If the excited atomic state has the same total angular momentum as the ground state (e.g. in alkalis, a $S_{1/2} \rightarrow P_{1/2}$ transition), then after they are fully polarized, the atoms stop absorbing light. Using this technique, nuclear vector polarizations of $97 \pm 1\%$ have been measured by the vanishing of fluorescence in $S_{1/2}$ to $P_{1/2}$ optical pumping as the ^{37}K atoms are polarized (see figure 12). An advantage of this technique is that the polarization of the same atoms that decay is continuously measured in a way that does not perturb the polarization. The neutrino asymmetry B_ν of ^{37}K has been measured to be $-0.755 \pm 0.020 \pm 0.013$, consistent with the Standard Model value with 3% error [115]. This is the first measurement of a neutrino asymmetry besides that of the neutron.

In these experiments, the atom cloud position and size are measured by photoionizing a small fraction of the atoms with a pulsed laser. The photoions are then accelerated and collected with the same apparatus that detects the β-decay recoils, making a three-dimensional image of the cloud. This is critical to test for different cloud position as a function of polarization state when the sign of the optical pumping is flipped, and is also critical for the absolute atom location for β–ν correlations [45, 115].

An additional novel observable is made possible by combining the polarized nuclei with the detection of the nuclear recoils. The spin asymmetry of slow-going recoils (i.e., back-to-back β–ν emission) vanishes in mixed Fermi/Gamow–Teller decays. This fact is independent of the Fermi/Gamow–Teller matrix element ratio, so it is independent of the degree of isospin mixing and the value of V_{ud}. Adequate statistics are difficult to obtain, but the observable is being measured at TRIUMF in the ^{37}K experiments.

Because of the ease of achieving high efficiency of recoil detection and characterizing the atom cloud pointlike source, it is natural in polarized β–ν coincidence measurements to consider the coefficient D of the time-reversal violating correlation from equation (3), $\hat{I} \cdot (\hat{p_\beta} \times \hat{p_\nu})$. Experiments have measured $D \leqslant 10^{-3}$ using distributed sources in ^{19}Ne [116] and the neutron [117]. This observable was immediately proposed after the discovery of parity violation [58]. Experiments in traps have been considered at TRIUMF, Berkeley, and KVI.

Spin asymmetry of recoils: search for tensor interactions. When parity violation was discovered, a large number of beta decay observables were suggested in the literature. Treiman noticed that the recoiling daughter nuclei from the β decay of polarized nuclei have average spin asymmetry $A_{\rm recoil} \approx 5/8\ (A_\beta + B_\nu)$. This vanishes in the allowed approximation for pure Gamow–Teller decays in the Standard Model, making it a sensitive probe of new interactions [118]. It is a very attractive experimental observable, because knowledge of the nuclear polarization at the 1–10% level is sufficient to be competitive.

Right-handed vector currents do not contribute, because they also cancel in the sum $(A_\beta + B_\nu)$. This leaves $A_{\rm recoil}$ uniquely sensitive to lepton–quark tensor interactions. A renormalizable interaction that Lorentz transforms like a tensor can be generated by the exchange of spin-0 leptoquarks [60].

Using the detection of shakeoff electrons to determine the recoil TOF and momentum, TRINAT has measured the recoil asymmetry with respect to the nuclear spin in ^{80}Rb, with result $A_{\rm recoil} = 0.015 \pm 0.029$ (stat) $\pm$ 0.019 (syst). The systematic error is limited by knowledge of first-order recoil corrections in this non-analog Gamow–Teller transition, which can be constrained by the dependence of $A_{\rm recoil}$ on recoil momentum. This result puts limits on a product of left-handed and right-handed tensor interactions that are complementary to the best ^{6}He β–ν correlation experiment [119].

2.4.3. Circularly polarized dipole force trap. One type of neutral atom trap only confines fully polarized atoms. A circularly polarized far-off resonant dipole force trap (CFORT) for Rb was efficiently loaded and demonstrated to achieve very high spin polarization at JILA in Boulder [120]. A dipole force trap from a diffraction-limited focused beam ordinarily traps atoms if it is tuned to the red of resonance, and expels them if tuned to the blue. If linearly polarized light is tuned just to the blue of the $S_{1/2} \rightarrow P_{1/2}$ (D1) resonance, it repels all the atoms. However, if the atoms are fully polarized, the coupling of circularly polarized light to the D1 transition vanishes. The same coupling coefficients apply as for real absorption, and the atoms already have maximum angular momentum and cannot absorb more. The light is still red detuned with respect to the D2 transition, so the fully polarized substate, and only that substate, is trapped. The quantization axis is defined by the laser light direction. This

trap is not limited by imperfect circular polarization, which merely makes the trap shallower (the spoiling of the polarization by stimulated Raman transitions is a negligibly small effect). TRINAT has worked on developing this trap in ^{39}K [121] for use in ^{37}K β decay experiments.

3. Weak interaction atomic physics

The traps also offer bright sources for Doppler-free spectroscopy, and precision measurements could measure the strength of weak neutral nucleon–nucleon and electron–nucleon interactions.

In broadest terms, higher-Z atoms are more sensitive to possible new short-ranged interactions between leptons and quarks, because the electron wavefunction overlap with the nucleus is larger. For atomic parity violation the effects scale like Z^2N with additional relativistic enhancement, anapole moments scale like $Z^{8/3}A^{2/3}$, and there is similar scaling for electric dipole moment effects. In case of parity-violation experiments, detailed knowledge of the atomic structure is necessary to extract the weak interaction physics from the measurement. Currently, only alkali atoms are sufficiently well understood theoretically. The combined requirements of high Z and alkali structure essentially single out francium as the best candidate for an atomic parity-violation experiment in that region. EDM research is still in the 'discovery phase', where the unambiguous identification is the primary goal; correspondingly, atomic structure knowledge is less relevant, and heavy stable elements such as mercury have played a dominant role. Nevertheless, EDMs are predicted to be significantly enhanced in the presence of nuclear octupole deformation, making certain radon and radium isotopes very interesting candidates for experiments. These considerations lead, rather accidentally, to the use of unstable isotopes for both parity violation and EDM experiments; i.e. unlike in β-decay measurements, the radioactivity is not essential, but an unavoidable result of choosing optimum atomic and nuclear properties.

Even with the availability of relatively copious amounts of the necessary isotopes from the present generation of radioactive beam facilities, such as ISAC at TRIUMF and ISOLDE at CERN, the number of atoms available for spectroscopy is orders of magnitude lower than for experiments with stable isotopes in beams or vapor cells. However, soon after the invention of laser trapping and cooling, it was realized that these new techniques could make up for this shortfall.

Experiments in this direction have been pursued at Stony Brook, where precision techniques were developed within a MOT environment to measure lifetimes and hyperfine splittings of several states. A review can be found in [122]. Several facilities plan work with radioactive atom traps, including Argonne National Lab, KVI Groningen, Legnaro, RCNP Osaka, and TRIUMF.

3.1. Searches for permanent electric dipole moments of electrons and nuclei

The existence of permanent electric dipole moments would violate time-reversal symmetry (for reviews see [123, 124]). The CPT theorem holds for locally Lorentz-invariant quantum field theories. Then CP violation implies time-reversal violation and vice versa. CP violation was observed in K meson decay in the 1960's and more recently in B meson decay. Most observables are consistent by the Wolfenstein parameterization of the CKM matrix phase. Electric dipole moments of the electron and the neutron are predicted to be very small within this Standard Model CP violation mechanism, and their existence at forseeable accuracy would imply non-Standard Model physics. The CP violation in the Standard Model is not enough to generate the baryon asymmetry of the universe in the method outlined by Sakharov [125].

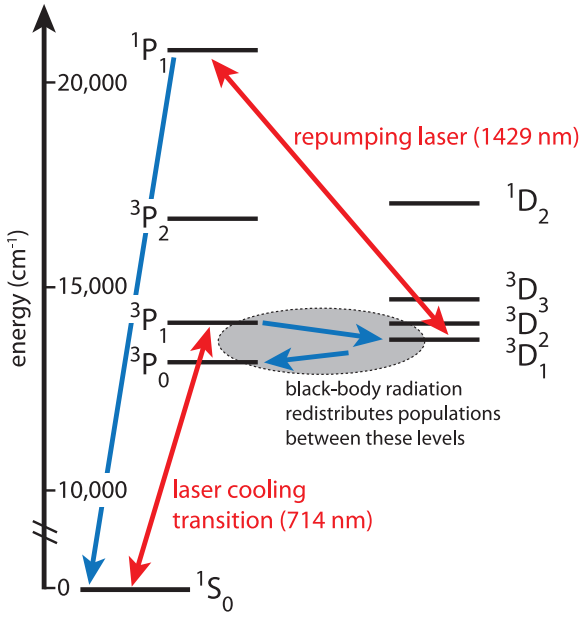

Figure 13. A level diagram for radium with the relevant states for laser trapping. Adapted and simplified from [25].

An electric dipole moment of the electron would manifest itself in the case of non-vanishing electronic angular momentum $J \neq 0$ as an atomic electric dipole moment. Although the effects are suppressed by the rearrangement of charge, when relativity is taken into account there remains an atomic electric dipole moment, and the effects are enhanced in heavier atoms.

A number of time-reversal violating effects can produce a nuclear 'Schiff moment' in $J = 0$ atoms. These include an electric dipole moment of the neutron or proton (or their constituent quarks) and time-reversal violating interactions. The nuclear Schiff moments are thought to be enhanced by octupole deformation [126], which is a well-established nuclear phenomenon. There are experiments underway to take advantage of this effect.

3.1.1. EDMs with radioactives in traps. Radium has now been trapped at Argonne National Lab [25]. The difficulty is great, so it is worth discussing some technical details here.

Radium was known to have a transition that could be pumped at high power by Ti:Sapph lasers, the $^1S_0 \rightarrow {}^3P_1$ transition at 714 nm (a level diagram is shown in figure 13). This transition appears to be spin forbidden, though in this heavy atom the configurations could possibly be mixed enough for it to be strong enough for trapping. Using an atomic beam, the Argonne group first measured the $^3P_1$ lifetime to be 420 ± 20 ns, adequately strong for trapping [24]. The ^{225}Ra is generated from a ^{229}Th source. A Zeeman slower was necessary to improve efficiency, as generally vapor cells do not work for alkaline earths.

The $^3P_1$ state has paths to decay to metastable $^3D_2$, $^3D_1$ and $^3P_0$ states. A repumping laser at 1429 nm was used to clear the $^3D_1$ state, extending trap lifetimes from milliseconds to seconds. Interesting effects from blackbody radiation acting as a repumper were observed that cleared the $^3P_0$ state [24]. The plan is to pursue an EDM measurement in the ^{225}Ra ground state

in a dipole force trap or lattice [24], taking advantage of well-characterized nuclear octupole enhancement in this particular isotope.

In addition to the ground state enhancements from the octupole deformation, there are potentially large enhancements in excited states of the radium atom. For example, the $^3D_2$ excited state, which is nearly degenerate in energy with the $^3P_1$ upper state of the trapping transition, has predicted EDM effects enhanced by nuclear Schiff and magnetic quadrupole moments by 10^5 over mercury, and nuclear anapole moment effects enhanced by 10^3 over cesium [23], though it remains to be seen whether the lifetime becomes too short when electric fields are applied to make this a practical system. The $^3D_1$ state has enhancements over francium for the atomic parity-violating E1 transition and electron EDM of 5 and 6, respectively [23].

KVI is building a MOT for barium atoms in preparation for a radium MOT using the stronger blue-frequency transition, eventually for EDM and atomic PV experiments [22, 127]. A group at RCNP [128] has plans for EDM experiments in francium, and is at the stage of measuring francium production.

Searches for an electron EDM is the goal of a fountain experiment by the group of Gould at LBNL, who have measured the scalar dipole polarizability of cesium [129]. They have published a prototype experiment to measure the electron EDM with a cesium atomic fountain [130] including characterization of systematic errors and an outline of upgrades needed to make it competitive. This group also developed the ^{229}Th source used for ^{221}Fr trapping at JILA [131]. At a radioactive beam facility francium could be trapped in similar numbers to stable cesium, and the higher-Z atom would enhance sensitivity by a factor of 8 [132].

A non-trap EDM experiment on radioactives. It does not involve a trap, but it is appropriate to mention work in a radon EDM experiment led by a University of Michigan group. The goal is to use the γ-ray anisotropies or β asymmetries as the Larmor precession probe to measure the EDM of octupole deformed radon isotopes, which could include ^{221}Rn, ^{223}Rn or ^{225}Rn. In preparation, spin-exchange optical pumping on ^{209}Rn was demonstrated at Stony Brook [133].

3.1.2. Trap efforts for EDMs in stable species. Laser-cooled atoms and traps have inspired EDM searches in reasonably high-Z non-radioactive systems. It is beyond the scope of this review to go beyond a simple mention of the possibilities.

Ytterbium has been trapped in Kyoto [33, 134] and Seattle [135], and groups in those places and at Bangalore [138] have proposed EDM experiments in this atom with relatively simple structure. Systematics for electron EDM experiments from collisions in a optical dipole force trap were considered originally in [136], while potential systematics for EDMs in a dipole force trap from light shifts were worked out in detail in [137]. Spin noise has been investigated in detail experimentally at Kyoto [139] and methods to minimize inhomogeneous broadening in optical dipole traps were proposed at Seoul [140], with EDM experiments in mind. There has also been work on EDM experiments using optical lattices in Cs [141, 142].

3.2. Atomic parity violation

Historically, atomic parity violation (APV) has played an important role. Shortly after the landmark e-D inelastic scattering experiment at SLAC [143, 144] measured the parity-violating part of the neutral current weak interaction, APV confirmed these findings at a very different momentum scale. In terms of the electron–quark coupling constants C_{1u} and C_{1d}, APV provides constraints nearly perpendicular to those of the SLAC experiment. A sequence of

increasingly refined APV experiments throughout the 1980s tightened these constraints to well below those of scattering experiments such as e-D at SLAC and e-carbon at BATES (see, e.g. the right panel in figure 16). Until the LEP collaborations published their results, APV even provided a competitive value for $\sin^2\theta_w$. This feat is no longer possible in the post-LEP era, but nevertheless low-energy experiments still have a key role to play. For example, when new states are discovered at the LHC, it will be important to know their couplings to the first generation of particles. Electrons and muons can be distinguished in the detectors, but up/down quark jets cannot be distinguished from jets of other generations. Atomic parity violation and other low-energy experiments are in a unique position to assist with this question. The challenge is to make them sensitive enough, which generally means part per thousand accuracy. We will describe below experiments in atomic parity violation in francium that are being designed to achieve this accuracy.

The study of weak interactions between nucleons gives unique information about very short-ranged correlations between them. Trapped francium atoms can be used to study a parity-violating electromagnetic moment, the anapole moment, that could provide conclusive information that these correlations change in nuclear matter.

3.3. Anapole moments: physics motivation

The strength of the weak neutral current in nuclear systems remains a puzzle. Historically, if the isovector weak meson–nucleon coupling f_π had been larger, weak neutral currents could have been discovered in low-energy nuclear experiments before Gargamelle's neutrino scattering.

The anapole ('not a pole') moment is a parity-violating electromagnetic moment produced by the weak nucleon–nucleon interaction. It is the result of the chirality acquired by the nucleon current that can be naively decomposed into two parts: a dipole moment, and a toroidal current that generates a magnetic field only in its interior (anapole). It is formally defined as

$$\mathbf{a} = -\pi \int \mathrm{d}^3 r\, r^2 \mathbf{J}(\mathbf{r}), \tag{4}$$

where $\mathbf{J}(\mathbf{r})$ is the electromagnetic current density in the nucleus. The nuclear anapole comes from a number of effects, though detailed calculations suggest it is dominated by core polarization by the valence nucleons [145]. This suggestion can be tested by a systematic study of francium isotopes with paired and unpaired neutrons.

The measurement of the ^{133}Cs anapole moment is difficult to reconcile with low-energy nuclear parity-violating experiments (figure 14). More cases are needed to understand the basic phenomenon, which is inherently interesting in itself. (It could be said that trying to understand nuclear magnetic moments from two cases would also be a difficult task.)

If the anapole moment values continue to disagree with lighter nuclei and few-nucleon systems [7], this could be due to the modification of the couplings in the nuclear medium [146]. The weak N–N interaction has recently been reformulated as an effective field theory, and this formalism provides a good framework in which to ask whether the effective couplings derived from few-body systems will be the same in heavier nuclei [146].

The result could have implications outside of the weak N–N interaction in another problem which has been reformulated as an effective field theory: a possible contribution to neutrinoless $\beta\beta$ decay from exchange of new heavy particles [148]. There are four-quark effective operators that are analogous with those in the weak N–N interaction, so the degree of renormalization of the weak N–N interaction could be an important guide to their computation. (See the last two pages of [146] for a discussion of this issue.)

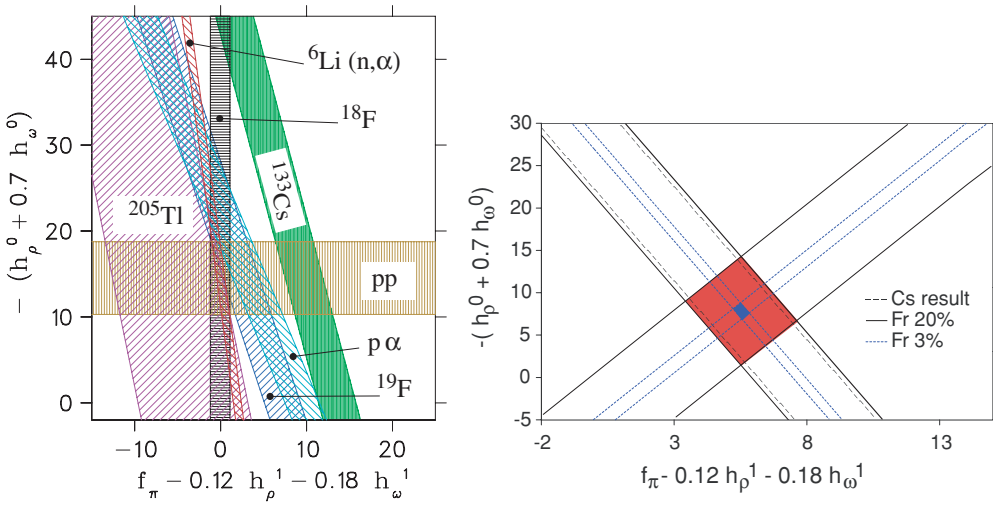

Figure 14. Left: constraints on isovector and isoscalar weak N-N couplings ($\times 10^7$) from measurement of the anapole moment of ^{133}Cs and natural thallium isotopes, compared to low-energy nuclear parity-violating experiments [7] including a recent accurate ^{6}Li(n,alpha) measurement [147]. Right: *projected* anapole moments of odd-neutron and even-neutron Fr isotopes would constrain isovector and isoscalar weak N–N couplings in the nuclear medium, if systematic measurements of the odd–even dependence in several francium isotopes successfully show that polarization of the core by the valence neutron is the main effect; courtesy E Gomez and L A Orozco.

3.3.1. Anapole moments: experimental overview. An anapole experiment in francium to be done at TRIUMF is currently in development by the FrPNC collaborators at the University of Maryland, William and Mary, San Luis Potosi, Manitoba and TRIUMF. The physics method is described in considerable detail in [149]. We only outline the technique here.

In the Boulder Cs and the Seattle Tl experiments, the anapole was extracted by determining the difference in the atomic parity-violation signal on two different hyperfine transitions ($nF \rightarrow n'F'$ and $nF' \rightarrow n'F$), i.e. taking the difference of two very similar numbers. As a result, the relative error on the anapole measurement is much larger than that of the nuclear-spin independent part. One way of addressing this problem is to measure atomic parity violation on a transition where the nuclear-spin independent part is absent, e.g. within a ground state hyperfine manifold, as was proposed long ago [150]. A PV-induced E1 transition between hyperfine states is driven by microwave radiation in a high-finesse cavity (see figure 15).

The M1 between these states is allowed and must be suppressed by orders of magnitude in contrast to the optical experiment (see below). Three simultaneous methods to do this are sketched broadly in figure 15. Together [149] estimates that the M1 amplitude can be reduced to less than 1% of the PV E1 amplitude (see figure 15).

Other efforts: anapole moments. DeMille at Yale is planning to measure anapole moments by placing diatomic molecules in a strong magnetic field [151]. A collaboration in Russia wants to measure the anapole moment in a potassium cell [152]. The Budker group in Berkeley has been pursuing measurements in ytterbium, which has many stable isotopes available [154], and with the appropriate hyperfine transitions could extract anapole moments. Other suggestions using atomic fountain techniques have recently appeared in the literature [155].

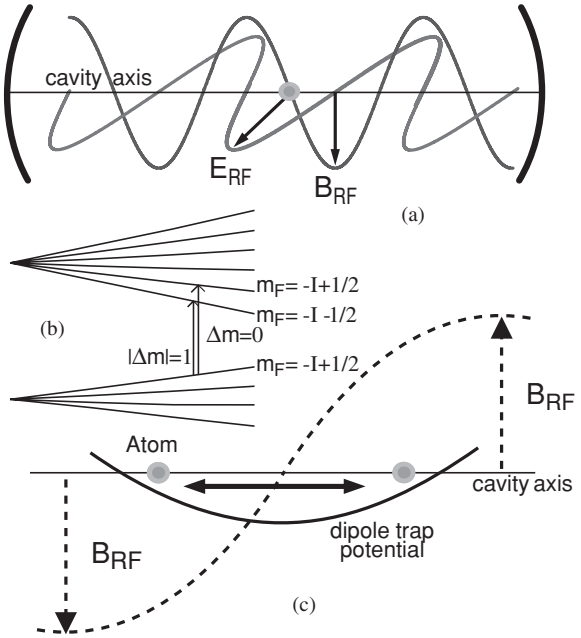

Figure 15. Schematic indications of the suppression of the allowed M1 transition in the anapole experiment. (a) The atoms are placed inside a microwave cavity containing a linearly polarized standing wave. By placing the atom cloud at the node of the magnetic field (and therefore the anti-node of the electric field), the amplitude of the M1 transition can be suppressed. (b) The Zeeman effect due to a static magnetic field applied along the direction of B_{RF} separates the frequency of the M1 transition ($\Delta m = 0$) from that of the E1 transition ($|\Delta m| = 1$), which is in resonance with the microwave radiation. This provides additional suppression of the M1. (c) In a finite-sized atom cloud, not all atoms can sit exactly at the node of the magnetic field. However, as long as the trap is precisely centered on the node, the M1 can be 'dynamically suppressed'. Individual atoms slosh back and forth through the trap center. Each time an atom crosses the node, it experiences a phase shift of π in the local oscillating magnetic field; if this happens sufficiently often during the coherent microwave excitation of the atom, a strong reduction in the M1 excitation rate can be achieved. Reprinted with permission from E Gomez *et al* [149], where more details are found. Copyright (2007) by the American Physical Society.

3.4. Atomic parity violation in francium: physics motivations

Atomic parity-violation measures the strength of the weak neutral current at very low momentum transfer. There are three types of such low-energy weak neutral current measurements with complementary sensitivity. The atomic weak charge is predominantly sensitive to the neutron's weak charge, as the proton weak charge is proportional to $1-4\sin^2\theta_W$, which accidentally is near zero. At Jefferson Lab, the upcoming Qweak electron scattering experiment on hydrogen is sensitive to the proton's weak charge. The SLAC E158 Moeller scattering is sensitive to the electron's weak charge. Different Standard Model extensions then contribute differently [157]. For example, the atomic parity weak charge is relatively insensitive to one-loop order corrections from all SUSY particles, so its measurement provides a benchmark for possible departures by the other 'low-energy' observables. As another example, Moeller scattering is purely leptonic and so has no sensitivity to leptoquarks, so the atomic parity weak charge can then provide the sensitivity to those. Figure 16 (right) from [158] shows the present constraints on weak quark couplings from parity-violating electron scattering and from atomic parity violation.

Figure 16 shows measurements of the Weinberg angle [157]. The low-energy experiments still have competitive sensitivity to certain specific Standard Model extensions compared to the LEP electroweak measurements—LEP's precision is better, but the low-energy experiments seeking terms interfering with the Z exchange can have inherently more sensitivity to tree-level exchange because they work on the tail of the Z resonance. It should be stressed that figure 16 cannot do justice to the highly complementary nature of the low-energy experiments, as it only plots the sensitivity to one Standard Model parameter, $\sin^2\theta_W$. Since Qweak and APV probe different quark combinations and E158 probes leptons, the sensitivities to physics beyond the SM are very different.

An explicit example is given by a recent review on constraints on new Z' bosons by Langacker [159]. Limits on the mass of new Z' bosons in several models and their mixing angle with the Standard Model Z are shown in [159, figure 1 and table 4]. The mixing angle constraints from 'global precision electroweak' fits are dominated by the LEP measurements at the Z pole, while the mass constraints come mainly from the low-energy atomic PV and electron scattering experiments. Those mass limits are at ≈600 GeV at 90% confidence, while direct searches at the Tevatron (assuming decays into Standard Model particles only) and at LEP 2 have recently reached better limits of ≈800 GeV. The mass reach of the low-energy measurements scales roughly with the square root of their accuracy, so improvements of 2–4 in accuracy would again provide useful information.

Constraints on parity-violating low-energy physics. Recently a new scalar particle with mass on the order of a few MeV, along with a new exchange boson with slightly greater mass, has been invoked to explain a possible excess of 511 keV photons at the galactic center. APV places severe constraints on parity-violating interactions at low energy, so it could immediately be concluded that the new exchange boson must have purely vector, parity-conserving couplings [160]. This demonstrates the power of the APV measurements to constrain exotic physics which can surprisingly evade all other constraints.

3.4.1. Status of atomic parity-violation measurements. The weak interaction in atoms induces a mixing of states of different parity, observable through APV measurements. Transitions that were forbidden due to selection rules become allowed through the presence of the weak interaction. The transition amplitudes are generally small and an interference method is commonly used to measure them. A typical observable has the form

$$|A_{\mathrm{PC}} + A_{\mathrm{PV}}|^2 = |A_{\mathrm{PC}}|^2 + 2Re(A_{\mathrm{PC}}A_{\mathrm{PV}}^*) + |A_{\mathrm{PV}}|^2, \tag{5}$$

where A_{PC} and A_{PV} represent the parity conserving and parity non-conserving amplitudes. The second term on the right side corresponds to the interference term and can be isolated because it changes sign under a parity transformation. The last term is usually negligible.

Most recent and on-going experiments in atomic PV rely on the large heavy nucleus (large Z) enhancement factor proposed by the Bouchiats ([161] is a recent review of PV prospects in hydrogen). These experiments follow two main strategies (see recent review by Bouchiat [162]). The first one is optical activity in an atomic vapor. This method has been applied to reach experimental precision of 2% in bismuth, 1.2% in lead and 1.2% in thallium.

The second strategy measures the excitation rate of a highly forbidden transition. The electric dipole transition between the $6s$ and $7s$ levels in cesium becomes allowed through the weak interaction. Interference between this transition and the one induced by the Stark effect due to the presence of an static electric field generates a signal proportional to the weak charge. The best atomic PV measurement to date uses this method to reach a precision of

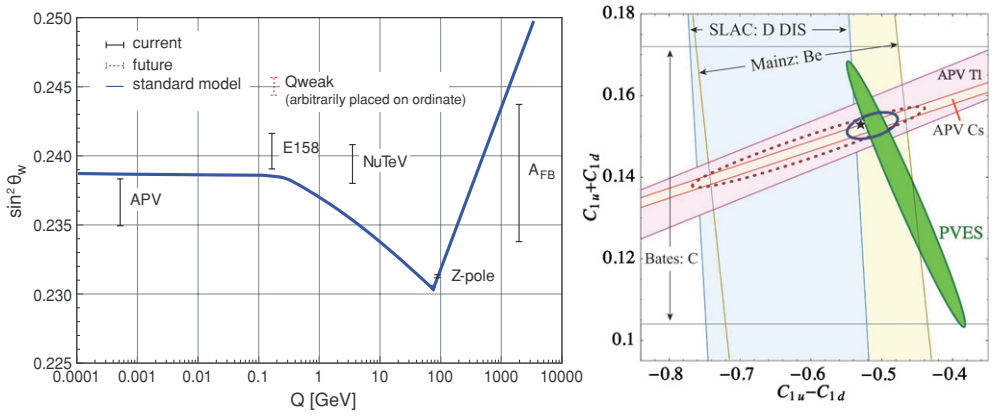

Figure 16. Left: measurements of the weak neutral current strength as a function of momentum transfer (θ_w is the Weinberg angle). Despite their lower precision, the low-energy experiments retain useful sensitivity to exchange of new bosons because they reside on the tail of the Standard Model Z resonance. Adapted from a figure, reprinted with permission from Erler J and Ramsey Musolf MJ [156]. Copyright (2005) by the American Physical Society. see also [156, 157]. The line is the Standard Model prediction. Right: constraints on weak quark couplings from electron scattering and atomic parity violation from [158], showing their complementarity. The star denotes the Standard Model prediction. (Note added in proof: a new atomic structure calculation for Cs has just been published [153], which reduces the overall uncertainty of the Cs APV result by about 30% and brings it into excellent agreement with the SM prediction.)

0.35% [5, 163, 164] (note a recent announcement of new calculations reducing the theory error further [153]).

Other methods have been proposed, and some work is already on the way. We have mentioned above Budker's work in optical transitions in ytterbium [154]. The Bouchiat group in Paris has worked on the highly forbidden 6s to 7s electric dipole transition in a cesium cell, but detects the occurrence of the transition using stimulated emission rather than fluorescence; this effort has ended after reaching 2.6% statistical accuracy [165].

Possible advantages for laser cooled and slowed atomic beams for APV studies have been considered by the Bouchiat group [166]. More recently, Bouchiat has suggested methods to measure anapole moments and electron–nucleon atomic PV by frequency shifts using fountains and atom interferometric methods, possibly working on as few at 10^4 atoms [155, 167]. These methods would avoid losses from two-photon ionization discussed below.

There are experimental efforts by the Fortson group in Seattle using a single barium ion and the KVI group using a single radium ion [168, 169].

The group at INFN in Legnaro has trapped ∼1000 Fr atoms in a MOT, and is considering atomic physics experiments including atomic parity violation [166, 170]. They have pioneered a number of innovative loading techniques [171] in stable Rb and are in the process of applying these to Fr. The FrPNC collaboration, in addition to the planned anapole measurement described above, is also working toward PV measurements in francium at TRIUMF.

This list is not intended to encompass all the efforts, but represents some of the groups interested in PV at present.

3.4.2. Atomic parity violation in francium: further experimental techniques. So far, there has been no parity-violation measurement in neutral atoms performed utilizing the new technologies of laser cooling and trapping. In order to create a road map for an experiment,

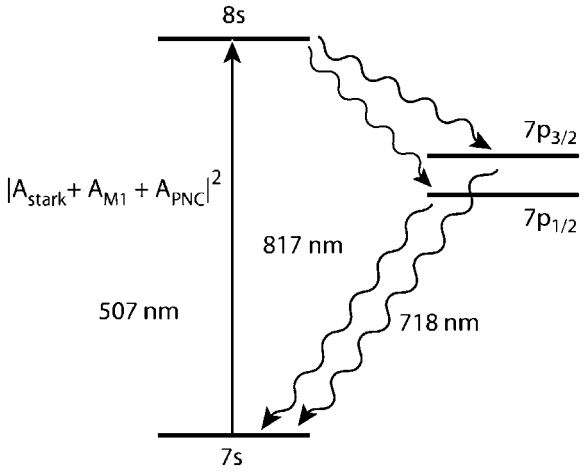

Figure 17. The most relevant atomic levels for Stark mixing experiments in francium.

one could assume a transition rate measurement following closely the technique used by the Boulder group in cesium [163, 164]. We start with a Stark shift to induce a parity conserving amplitude between the 7s and 8s levels of francium, and look how this electromagnetic term will interfere with the weak interaction amplitude (equation (5)). This gives rise to a left–right asymmetry with respect to the system of coordinates defined by the static electric field **E**, static magnetic field **B** and the Poynting vector **S** of the excitation field, such that the observable is proportional to $\mathbf{B} \cdot (\mathbf{S} \times \mathbf{E})$.

Francium atoms would accumulate in a magneto-optic trap (MOT). Then, after further cooling to control their velocities, they would be transferred to another region where a dipole trap will keep them ready for the measurement. After being optically pumped to one hyperfine state, the atoms would be exposed to an intense standing wave mode of 507 nm light resonant with the 7s to 8s transition, in the presence of a dc electric field. Excited atoms will decay via the 7p state to populate the empty hyperfine state. Optical pumping techniques allow one to recycle the atom that has performed the parity non-conserving transition many times enhancing the probability to detect the signature photon.

3.4.3. Ramping up to atomic PV: 'Forbidden' M1 in atomic francium. The strength of the 'forbidden' M1 in atomic francium is sensitive to relativistic corrections to many-body perturbation theory [172]. These effects are useful tests of the atomic theory needed to extract weak coupling coefficients from atomic parity-violation experiments. Thus a logical precursor to any optical APV experiment in francium is the spectroscopy of the 7s $\rightarrow$ 8s transition (see figure 17). The line is best located by driving the Stark-induced amplitude in a strong electric field (several kV cm^{-1}) in a configuration of parallel external field and laser polarization, where the large scalar transition polarizability α provides a (relatively) strong signal. With crossed field and polarization, the 30 times weaker transitions characterized by the vector transition polarizability β then allows us to determine the ratio α/β. Observing the E1–M1 interference by flipping fields similar to the APV procedure, produces intensity modulation at the 1% level, about a hundred times larger than the modulation expected in APV. The quality of this signal will be a crucial indicator for the prospects of observing a 10^{-4} modulation to better than 1%—the eventual goal for APV.

3.4.4. Signal-to-noise ratio for atomic parity violation. To estimate the requirements for a parity-violation measurement in francium it is good to take the Boulder Cs experiment as a guide [163, 164]. The most important quantity to estimate is the signal-to-noise ratio since that will determine many of the requirements of the experiment. The approach of Stark mixing works as an amplifier in the full sense of the word, it enlarges the signal, but it also brings noise. The Stark-induced, parity conserving part $|A_{\mathrm{PC}}|^2$ not only dominates the transition strength, it also contributes essentially all of the shot noise to the measurement. The number of excitations in a sample of N atoms is given (up to an angular momentum factor of order one depending on geometry and polarization) by

$$S_{\mathrm{stark}} = \frac{2}{c\hbar^2\epsilon_0} I\tau(\beta E)^2 N; \tag{6}$$

the parity-violation signal is

$$S_{\mathrm{PV}} = \frac{2}{c\hbar^2\epsilon_0} I\tau 2E\beta\,\mathrm{Im}(E_{\mathrm{PV}})N, \tag{7}$$

where β is the vector Stark polarizability, E is the dc electric field used for the Stark mixing, $\mathrm{Im}(E_{\mathrm{PV}})$ is the parity-violating amplitude, τ is the lifetime of the upper s-state, and I the intensity of the excitation source. The polarizabilities are quoted exclusively in atomic units in the literature, and the corresponding value in SI units is obtained by $\beta_{\mathrm{SI}} = \beta_{au}/6.06510 \times 10^{40}$. Since the Stark rate dominates by orders of magnitude, and assuming only shot noise as the dominant source of noise, the signal-to-noise ratio achieved in 1 s is

$$\frac{S_{\mathrm{PV}}}{N_{\mathrm{noise}}} = 2\sqrt{\frac{2I\tau N}{c\hbar^2\epsilon_0}}\mathrm{Im}(E_{\mathrm{PV}}). \tag{8}$$

The calculated value from Dzuba *et al* [173] for $\mathrm{Im}(E_{\mathrm{PV}})$ of 1.5×10^{-10} in atomic units is 18 times larger than in cesium.

A serious complication for a trap-based experiment is photoionization in the excited state by the intense 507 nm radiation, which was already discussed in [174]. At intensities of 800 kW cm^{-2} as used by Wood *et al* [163, 164], the probability for photoionization per excitation was 10%. In a beam experiment, where each atom is used only once, this is not particularly concerning. In a trap scenario, each atoms must be re-used over a time span of up to seconds, and hence, the photoionization rate must be brought down to a compatible level (accidentally, in Fr the situation is worse, as the 507 nm light can ionize into the continuum from both the 8s and the $7p_{3/2}$ states). This can be remedied by reducing the light intensity by a factor of 300, which will bring the photoionization rate down to about 1 Hz, yielding a 7s–8s excitation rate of 30 Hz per atom. For guidance, we can refer to the Cs experiment which had a 6s–7s excitation rate of 10^{10} Hz and find that 3×10^8 trapped atoms lead to the same signal, but the fluorescence modulation upon parity reversals is 2×10^{-4}, about an order of magnitude larger. The signal to noise is then

$$S/N = 2 \times 10^{-4}\sqrt{30tN},$$

where t is the observation time in seconds and N the number of atoms in the trap. Or, the time to obtain a S/N with a certain excitation rate R and N atoms in the trap and an asymmetry A is

$$t = \frac{(S/N)^2}{A^2RN}.$$

Based on these purely statistical considerations, a 1.0% APV measurement requires about 2.5 h using 10^6 trapped atoms; ten times more atoms would allow a 0.1% test in 25 h. Naturally, much more time has to be spent to deal with systematic effects.

3.4.5. Neutron radius question. Since the weak charge in atoms stems mostly from the neutrons, there is some dependence on the neutron distribution in the nucleus, a quantity with few reliable experimental probes. The neutron radius measurement with parity-violating electron scattering at Jefferson Lab ('PRex' [175]) would result in an uncertainty on the weak charge in ^{212}Fr of 0.2% [176]. Isotopic ratios would need a next generation neutron radius experiment [176], though a recent analysis suggests that when cancellations in correlated nuclear theory errors are taken into account, new physics can indeed by extracted by measuring chains of isotopes [177], which also have the potential to remove much of the atomic theory uncertainty.

Work at Stony Brook investigated the hyperfine anomaly in $^{208-212}$Fr [178]. Different atomic wavefunctions have different overlap with the nucleus, so a changing spatial distribution of nuclear magnetism will change the relative hyperfine splittings. For the odd-neutron isotopes, this effect is sensitive to the spatial wavefunction of the valence neutron, in a manner similar to magnetic multipoles in electron scattering. This effect will be measured in the chain of francium isotopes in an upcoming experiment at TRIUMF [179].

4. Conclusion

Neutral atom traps provide unique environments for precision experiments using radioactive isotopes. The first trap-based measurements in β decay have been completed, and the results are improving constraints on interactions beyond the Standard Model. The ability to measure the momentum of the daughter nuclear recoils has produced two of the best β–ν correlation experiments. Adding the ability to reverse the spin of highly polarized atoms leads to unique observables with the potential to improve parity and time-reversal violation tests in β decay.

Results from francium atomic spectroscopy have long been in evidence. Plans are proceeding to harness the trapping technologies to measure weak neutral current effects in atoms and nuclei. By storing individual atoms for seconds, a sufficient sample of radioactive atoms can be provided with realistic production rates at radioactive beam facilities. The challenge will be to understand and control systematic errors in an online environment. Several labs have plans for time-reversal-violating electric dipole moment searches in radium, radon and francium. Undoubtedly, these efforts will produce exciting new results in coming years.

Acknowledgments

This work was supported by the Natural Sciences and Engineering Council of Canada and National Research Council Canada through TRIUMF. J B thanks innumerable TRINAT collaborators whose work appears here, in particular O Häusser. G G thanks S A Page. G G and J B thank G D Sprouse and L A Orozco.

References

[1] Sprouse G D and Orozco L A 1997 Laser trapping of radioactive atoms *Annu. Rev. Nucl. Part. Sci.* **47** 429
[2] Kozlov Yu V *et al* 2006 The WITCH experiment: towards weak interactions studies. Status and prospects *Hyperfine Interact.* **172** 15
[3] Fléchard X *et al* 2008 Paul trapping of radioactive ^{6}He^{+} ions and direct observation of their β decay *Phys. Rev. Lett.* **101** 212504
[4] Scielzo N, Levand A, Savard G, Tanihata I, Zabransky B, Clark J, Sharma H, Sharma K and Wang Y 2005 Precision β-decay studies in a RFQ ion trap *Bull. Am. Phys. Soc.* DNP CH.00009

[5] Bennett S C and Wieman C E 1999 Measurement of the 6S → 7S transition probability in atomic cesium and an improved test of the Standard Model *Phys. Rev. Lett.* **82** 2484

[6] Anthony P L *et al* 2005 Precision measurement of the weak mixing angle in Møller scattering *Phys. Rev. Lett.* **95** 081601

[7] Haxton W C, Liu C-P and Ramsey-Musolf M 2002 *Phys. Rev.* C **65** 045502
Haxton W C and Wieman C E 2001 *Annl. Rev. Nucl. Part. Sci.* **51** 261
Haxton W C, Liu C-P and Ramsey-Musolf M 2001 *Phys. Rev. Lett.* **86** 5247

[8] Raab E L, Prentiss M, Alex Cable, Chu S and Pritchard D E 1987 Trapping of neutral sodium atoms with radiation pressure *Phys. Rev. Lett.* **59** 2631

[9] Ashkin A and Gordon J P 1983 Stability of radiation-pressure particle traps: an optical Earnshaw theorem *Opt. Lett.* **8** 511

[10] Pritchard D E and Ketterle W 1992 Atom traps and atom optics *Proc. Int. School of Physics Enrico Fermi CXVIII* ed E Arimondo, W D Phillips and F Strumia
Chu S 1992 Laser cooling and manipulation of atoms, and selected applications *Proc. of the Int. School of Physics Enrico Fermi CXVIII* ed E Arimondo, W D Phillips and F Strumia

[11] Chu S, Bjorkholm J E, Ashkin A and Cable A 1986 Experimental observation of optically trapped atoms *Phys. Rev. Lett.* **57** 314

[12] Grimm R, Weidemüller M and Ovchinnikov Y B 2000 Optical dipole traps for neutral atoms *Adv. Atom. Mol. Opt. Phys.* **42** 95

[13] Goepfert A, Bloch I, Haubrich D, Lison F, Schütze R, Wynands R and Meschede D 1997 Stimulated focusing and deflection of an atomic beam using picosecond laser pulses *Phys. Rev.* A **56** R3354

[14] Söding J, Grimm R, Ovchinnikov Yu B, Bouyer Ph and Salomon Ch 1997 Short-distance atomic beam deceleration with a stimulated light force *Phys. Rev. Lett.* **78** 1420

[15] Partlow M, Miao X, Bochmann J, Cashen M and Metcalf H 2004 Bichromatic slowing and collimation to make an intense helium beam *Phys. Rev. Lett.* **93** 213004

[16] Chu S 1998 Manipulation of neutral particles *Rev. Mod. Phys.* **70** 685

[17] Bergeman T, Erez G and Metcalf H 1987 Magnetostatic trapping fields for neutral atoms *Phys. Rev.* A **35** 1535

[18] Walker T, Feng P, Hoffmann D and Williamson R S III 1992 Spin-polarized spontaneous-force atom trap *Phys. Rev. Lett.* **69** 2168

[19] Balykin V I, Minogin V G and Letokhov V S 2000 Electromagnetic trapping of cold atoms *Rep. Prog. Phys.* **63** 1429

[20] Kofoed-Hansen O 1954 Theoretical angular correlations in allowed beta transitions *Dan. Mat. Fys. Medd.* **28** 1

[21] Swanson T B, Asgeirsson D, Behr J A, Gorelov A and Melconian D 1998 Efficient transfer in a double magneto-optical trap system *J. Opt. Soc. Am.* B **15** 2641

[22] De S, Dammalapati U, Jungmann K and Willmann L 2008 Magneto optical trapping of Barium arXiv:0807.4100

[23] Dzuba V A, Flambaum V V and Ginges J S M 2000 Calculation of parity and time invariance violation in the radium atom *Phys. Rev.* A **61** 062509

[24] Scielzo N D, Guest J R, Schulte E C, Ahmad I, Bailey K, Bowers D L, Holt R J, Lu Z-T, O'Connor T P and Potterveld D H 2006 Measurement of the lifetimes of the lowest $^3P^1$ state of neutral Ba and Ra *Phys. Rev.* A **73** 010501

[25] Guest J R, Scielzo N D, Ahmad I, Bailey K, Greene J P, Holt R J, Lu Z-T, O'Connor T P and Potterveld D H 2007 Laser trapping of ^{225}Ra and ^{226}Ra with repumping by room-temperature blackbody radiation *Phys. Rev. Lett.* **98** 093001

[26] Wang L-B *et al* 2004 Laser spectroscopic determination of the ^{6}He nuclear charge radius *Phys. Rev. Lett.* **93** 142501

[27] Mueller P *et al* 2007 Nuclear Charge Radius of ^{8}He *Phys. Rev. Lett.* **99** 252501

[28] Chen C Y, Li Y M, Bailey K, O'Connor T P, Young L and Lu Z-T 1999 Ultrasensitive isotope trace analyses with a magneto-optical trap *Science* **286** 1139

[29] Shimizu F 1991 *Jpn. J. Appl. Phys.* **60** 864
Shimizu F 1990 *Chem. Phys.* **145** 327

[30] Adams C S and Riis E 1997 Laser cooling and trapping of neutral atoms *Prog. Quantum Electron.* **21** 1

[31] Uhlenberg G, Dirscherl J and Walther H 2000 Magneto-optical trapping of silver atoms *Phys. Rev.* A **62** 063404

[32] Bell A S, Stuhler J, Locher S, Hensler S, Mlynek J and Pfau T 1999 A magneto-optical trap for chromium with population repumping via intercombination lines *Europhys. Lett.* **45** 156

[33] Honda K, Takahashi Y, Kuwamoto T, Fujimoto M and Toyoda K 1999 Magneto-optical trapping of Yb atoms and a limit on the branching ratio of the $^1P_1$ state *Phys. Rev.* A **59** R934

[34] Hachisu H, Miyagishi K, Porsev S G, Derevianko A, Ovsiannikov V D, Pal'chikov V G, Takamoto M and Katori1 H 2008 Trapping of neutral mercury atoms and prospects for optical lattice clocks *Phys. Rev. Lett.* **100** 053001

[35] McClelland J J and Hanssen J L 2006 Laser cooling without repumping: a magneto-optical trap for erbium atoms *Phys. Rev. Lett.* **96** 143005

[36] Berglund A J, Hanssen J L and McClelland J J 2008 Narrow-line magneto-optical cooling and trapping of strongly magnetic atoms *Phys Rev. Lett.* **100** 113002

[37] Kumita T, Hirose T, Irako M, Kadoya K, Matsumoto B, Wada K, Mondal N N, Yabu H, Kobayashi K and Kajita M 2002 Study on laser cooling of ortho-positronium *Nucl. Instrum. Methods Phys. Res.* B **192** 171

[38] Mills A P Jr 2002 Positronium molecule formation, Bose–Einstein condensation, and stimulated annihilation *Nucl. Instrum. Methods Phys. Res.* B **192** 107

[39] Gwinner G, Behr J A, Cahn S B, Ghosh A, Orozco L A, Sprouse G D and Xu F 1994 Magneto-Optic Trapping of Radioactive ^{79}Rb *Phys. Rev. Lett.* **72** 3795

[40] Behr J A, Cahn S B, Dutta S B, Ghosh A, Gwinner G, Holbrow C H, Orozco L A, Sprouse G D, Urayama J and Xu F 1994 A low-energy ion beam from alkali heavy-ion reaction products *Nucl. Instrum. Methods Phys. Res.* A **351** 256

[41] Swenson D R and Anderson L W 1988 Relaxation rates for optically pumped Na vapor on silicone surfaces *Nucl. Instrum Methods Phys. Res.* B **29** 627

[42] Fedchak J, Cabauy P, Cummings W, Jones C and Kowalczyk R 1997 Silane coatings for laser-driven polarized hydrogen sources and targets *Nucl. Instrum. Methods Phys. Res.* A **391** 405

[43] Holbrow C H, Ghosh A P, Heinzen D, Zhu X, Quivers W W Jr, Shimkaveg G, Pappas P G, Thomas J E and Feld M S 1986 Complete Doppler coverage in laser optical pumping by wall-induced velocity-changing collisions *Phys. Rev.* A **34** 2477

[44] Lu Z-T, Bowers C, Freedman S J, Fujikawa B K, Mortara J L, Shang S-Q, Coulter K P and Young L 1994 Laser trapping of short-lived radioactive isotopes *Phys. Rev. Lett.* **72** 3791

[45] Gorelov A *et al* 2005 Scalar interaction limits from the β-ν correlation of trapped radioactive atoms *Phys. Rev. Lett.* **94** 142501

[46] Dombsky M, Bishop D, Bricault P, Dale D, Hurst A, Jayamanna K, Keitel R, Olivo M, Schmor P and Stanford G 2000 Commissioning and initial operation of a radioactive beam ion source at ISAC *Rev. Sci. Instrum.* **71** 978

[47] Guckert R, Zhao X, Crane S G, Hime A, Taylor W A, Tupa D, Vieira D J and Wollnik H 1998 Magneto-optical trapping of radioactive ^{82}Rb atoms *Phys. Rev.* A **58** R1637

[48] Stephens M, Rhodes R and Wieman C 1994 Study of wall coatings for vapor-cell laser traps *J. Appl. Phys.* **76** 3479

[49] DiRosa M D, Crane S G, Kitten J J, Taylor W A, Vieira D J and Zhao X 2003 Magneto-optical trap and mass-separator system for the ultra-sensitive detection of ^{135}Cs and ^{137}Cs *Appl. Phys.* B **76** 45

[50] Anderson B P and Kasevich M A 1994 Enhanced loading of a magneto-optic trap from an atomic beam *Phys. Rev.* A **50** R3581

[51] Rasel E, Pereira Dos Santos F, Saverio Pavone F, Perales F, Unnikrishnan C S and Leduc M 2004 White light transverse cooling of a helium beam *Eur. Phys. J.* **7** 1434

[52] Marinelli C, Nasyrov K A, Bocci S, Pieragnoli B, Burchianti A, Biancalana V, Mariotti E, Atutov S N and Moi L 2001 A new class of photo-induced phenomena in siloxane films *Eur. Phys. J.* D **13** 231

[53] Severijns N, Beck N and Naviliat-Cuncic O 2006 Tests of the standard electroweak model in beta decay *Rev. Mod. Phys.* **78** 991

[54] Lee T D and Yang C N 1956 Question of parity conservation in weak interactions *Phys. Rev.* **104** 254

[55] Steven Weinberg 1958 Charge symmetry of weak interactions *Phys. Rev.* **112** 1375

[56] Ormand W E, Brown B A and Holstein B R 1989 Limits on the presence of scalar and induced-scalar currents in superallowed β decay *Phys. Rev.* C **40** 2914

[57] Holstein B 1984 Recoil effects in allowed beta decay: the elementary particle approach *Rev. Mod. Phys.* **46** 789
Holstein B 1984 Recoil effects in allowed beta decay: the elementary particle approach *Rev. Mod. Phys.* **48** 673 (erratum)

[58] Jackson J D, Treiman S B and Wyld H W 1957 Possible tests of time reversal invariance in beta decay *Phys. Rev.* **106** 517

[59] Profumo S, Ramsey-Musolf M J and Tulin S 2007 Supersymmetric contributions to weak decay coefficients *Phys. Rev.* D **75** 075017

[60] Herczeg P 2001 Beta decay beyond the Standard Model *Prog. Part. Nucl. Phys.* **46/2** 413

[61] Hardy J C and Towner I S 2005 Superallowed $0^+ \rightarrow 0^+$ nuclear β decays: a critical survey with tests of the conserved vector current hypothesis and the Standard Model *Phys. Rev.* C **71** 055501

[62] Adelberger E G 1993 Improved limits on scalar weak couplings *Phys. Rev. Lett.* **70** 2856
Adelberger E G 1993 Improved limits on scalar weak couplings *Phys. Rev. Lett.* **71** 469 (erratum)

[63] Adelberger E G, Ortiz C, Garcia A, Swanson H E, Beck M, Tengblad O, Borge M J G, Martel I and Bichsel H (the ISOLDE Collaboration) 1999 Positron-neutrino correlation in the $0^+ \rightarrow 0^+$ decay of ^{32}Ar *Phys. Rev. Lett.* **83** 1299
Adelberger E G, Ortiz C, Garcia A, Swanson H E, Beck M, Tengblad O, Borge M J G, Martel I and Bichsel H *Op cit.* 3101 (erratum)

[64] Garcia A 2008 Electron-neutrino correlation and Isospin breaking in $0^+ \rightarrow 0^+$ decay of ^{32}Ar (and Vud from neutron decay) *4th RIA Physics Workshop, INT Seattle* and http://www.int.washington.edu/talks/WorkShops/int_07_36W

[65] Campbell Bruce A and Maybury David W 2005 Constraints on scalar couplings from $\pi^{\pm} \rightarrow l^{\pm}\nu_l$ *Nucl. Phys.* B **709** 419

[66] Ito Takeyasu M and Prézeau Gary 2005 Neutrino mass constraints on β Decay *Phys. Rev. Lett.* **94** 161802

[67] Scielzo N D, Freedman S J, Fujikawa B K and Vetter P A 2004 Measurement of the β-ν correlation using magneto-optically trapped ^{21}Na *Phys. Rev. Lett.* **93** 102501

[68] Iacob V E *et al* 2006 Branching ratios for the beta decay of ^{21}Na *Phys. Rev.* C **74** 015501

[69] Weiner J, Bagnato V S, Zilio S and Julienne P S 1999 Experiments and theory in cold and ultracold collisions *Rev. Mod. Phys.* **71** 1

[70] DeMille D 2002 Quantum computation with trapped polar molecules *Phys. Rev. Lett.* **88** 067901

[71] Vetter P, Abo-Shaeer J R, Freedman S J and Maruyama R 2008 Measurement of the β-ν correlation of ^{21}Na using shakeoff electrons *Phys. Rev.* C **77** 035502

[72] Walhout M, Sterr U and Rolston S L 1996 Magnetic inhibition of polarization-gradient laser cooling in $\sigma^+ - \sigma^-$ optical molasses *Phys. Rev.* A **54** 2275

[73] Scielzo N D, Freedman S J, Fujikawa B K and Vetter P A 2003 Recoil-ion charge-state distribution following the β^+ decay of ^{21}Na *Phys. Rev.* A **68** 022716

[74] Carlson T A, Pleasonton F and Johnson C H 1963 Electron shake off following the β^- decay of He^6 *Phys. Rev.* **129** 2220
Carlson T A, Nestor C W Jr, Thomas T and Malik F B 1968 Calculation of electron shake-off for elements from Z = 2 to 92 with the use of self-consistent-field wave functions *Phys. Rev.* **169** 27

[75] Behr J A *et al* 2005 Weak interaction symmetries with atom traps *Eur. Phys. J.* A **25** 685–89

[76] Commins E D and Bucksbaum P H 1983 *Weak Interactions of Leptons and Quarks* (Cambridge: Cambridge University Press)

[77] Gluck F 1998 Order-α radiative correction to ^{6}He and ^{32}Ar β decay recoil spectra *Nucl. Phys.* A **628** 493
Johnson C H, Pleasonton F and Carlson T A 1963 Precision measurements of the recoil energy spectrum from the decay of He^6 *Phys. Rev.* **132** 1149

[78] Stratowa Chr, Dobrozemsky R and Weinzieri P 1978 Ratio $|g_A/g_V|$ derived from the proton spectrum in free-neutron decay *Phys. Rev.* D **18** 3970

[79] Allen J S, Burman R L, Hermannsfeldt W B, Stähelin P and Braid T H 1959 Determination of the beta-decay interaction from electron-neutrino angular correlation measurements *Phys. Rev.* **116** 134

[80] Feynman R P and Gell-Mann M 1958 Theory of the Fermi interaction *Phys. Rev.* **109** 193

[81] Behr J A 2005 (spokesman) Upgrade of ^{38m}K β-ν correlation TRIUMF proposal S1070 (http://www.triumf.info/facility/experimenters/expdb/public.php)

[82] Calaprice F P 1975 Second class interactions and the electron-neutrino correlation in nuclear beta decay *Phys. Rev.* C **12** 2016

[83] Trinczek M *et al* 2003 Novel Search for heavy ν mixing from the β^+ decay of ^{38m}K confined in an atom trap *Phys. Rev. Lett.* **90** 012501

[84] Lu Z-T 2008 private communication

[85] Scielzo N D, Freedman S J, Fujikawa B K, Kominis I, Maruyama R, Vetter P A and Vieregg J R 2004 Detecting shake-off electron-ion coincidences to measure β-decay correlations in laser trapped ^{21}Na *Nucl. Phys.* A **746** 677c

[86] Amsler C *et al* 2008 The review of particle physics *Phys. Lett.* B **667** 1

[87] Abazajian K, Fuller George M and Patel M 2001 Sterile neutrino hot, warm, and cold dark matter *Phys. Rev.* D **64** 23501

[88] Dolgov A D, Hansen S H, Raffelt G and Semikoz D V 2000 Heavy sterile neutrinos: bounds from big-bang nucleosynthesis and SN 1987A *Nucl. Phys.* B **590** 562

[89] McLaughlin G C and Ng J N 2001 Use of nuclear β decay as a test of bulk neutrinos in extra dimensions *Phys. Rev.* D **63** 053002

[90] Deutsch J, Lebrun M and Prieels R 1990 Searches for admixture of massive neutrinos into the electron flavour *Nucl. Phys.* A **518** 149

[91] Ullrich J, Moshammer R, Born A, Dörner R, Schmidt L Ph H and Schmidt-Böcking H 2003 Recoil-ion and electron momentum spectroscopy: reaction-microscopes *Rep. Prog. Phys.* **66** 1463
Dörner R, Mergel V, Jagutzki J, Spielberger L, Ullrich J, Moshammer R and Schmidt-Böcking H 2000 Cold target recoil ion momentum spectroscopy: a 'momentum-microscope' to view atomic collision dynamics *Phys. Rep.* **330** 95

[92] Beacom J F and Yüksel H 2006 Stringent constraint on galactic positron production *Phys. Rev. Lett.* **97** 071102

[93] Berezhiani Z, Gianfagna L and Giannotti M 2001 Strong CP problem and mirror world: the Weinberg–Wilczek axion revisited *Phys. Lett.* B **500** 286

[94] Hall L and Watari T 2004 Electroweak supersymmetry with an approximate U(1) Peccei-Quinn symmetry *Phys. Rev.* D **70** 115001

[95] Derbin A V, Egorov A I, Mitropolsky I A and Muratova V N 2005 Search for solar axions emitted in an M1 transition in ^{7}Li nuclei *JETP Lett.* **81** 356
Derbin A V, Egorov A I, Mitropolsky I A, Muratova V N, Bakhlanov S V and Tukhkonen L M 2002 Search for Axions Emitted in Nuclear Magnetic Transitions *Phys. At. Nuclei* **65** 1302

[96] Minowa M, Inoue Y and Asanuma T 1993 Invisible axion search in ^{139}La M1 transition *Phys. Rev. Lett.* **71** 4120

[97] Dodelson S and Widrow L M 1994 Sterile neutrinos as dark matter *Phys. Rev. Lett.* **72** 17
Giudice G F, Kolb E W, Riotto A, Semikoz D V and Tkachev II 2001 Standard model neutrinos as warm dark matter *Phys. Rev.* D **64** 043512

[98] Abazajian K and Koushiappas S M 2006 Constraints on sterile neutrino dark matter *Phys. Rev.* D **74** 023527

[99] Kusenko A 2004 Pulsar kicks from neutrino oscillations *Int. J. Mod. Phys.* D **13** 2065

[100] Fryer C L and Kusenko A 2006 Effects of neutrino-driven kicks on the supernova explosion mechanism *Astrophys. J. Suppl. Ser.* **163** 335

[101] Asaka T, Blanchet S and Shaposhnikov M 2005 The νMSM, dark matter and neutrino masses *Phys. Lett.* B **631** 151
Asaka T and Shaposhnikov M 2005 The νMSM, dark matter and the baryon asymmetry of the universe *Phys. Lett.* B **620** 17
Shaposhnikov M and Tkachev I 2006 The νMSM, Inflation, and Dark Matter *Phys. Lett.* B **639** 414

[102] Gelmini G, Palomares-Ruiz S and Pascoli S 2004 Low reheating temperatures and the visible sterile neutrino *Phys. Rev. Lett.* **93** 081302

[103] Boyarsky A, Neronov A, Ruchayskiy O and Shaposhnikov M 2005 Constraints on sterile neutrinos as dark matter candidates from the diffuse X-ray background *Mon. Not. R. Astron. Soc.* **370** 213

[104] Bezrukov F and Shaposhnikov M 2007 Searching for dark matter sterile neutrinos in the laboratory *Phys. Rev.* D **75** 053005

[105] Price G N, Bannerman S T, Viering K, Narevicius E and Raizen M G 2008 Single-photon atomic cooling *Phys. Rev. Lett.* **100** 093004

[106] Hogan S D, Wiederkehr A W, Schmutz H and Merkt F 2008 Magnetic trapping of hydrogen after multistage Zeeman deceleration *Phys. Rev. Lett.* **101** 143001

[107] Abachi S *et al* 1996 Search for right-handed W bosons and heavy W' in proton-antiproton collisions at sqrt[s] = 1.8 TeV *Phys. Rev. Lett.* **76** 3271

[108] Langacker P and Uma Sankar S 1989 Bounds on the mass of W_R and the W_L-W_R mixing angle ζ in general $SU(2)_L \times SU(2)_R \times U(1)$ models *Phys. Rev.* D **40** 1569

[109] Thomas E *et al* 2001 Positron polarization in the decay of polarized ^{12}N: a precision test of the Standard Model *Nucl. Phys.* A **694** 559

[110] Wilkinson D H 2000 Limits to second-class nucleonic and mesonic currents *Eur. Phys. J.* A **7** 307

[111] Rowe M A, Freedman S J, Fujikawa B K, Gwinner G, Shang S-Q and Vetter P A 1999 Ground-state hyperfine measurement in laser-trapped radioactive ^{21}Na *Phys. Rev. Lett.* **59** 1869

[112] Crane S G, Brice S J, Goldschmidt A, Guckert R, Hime A, Kitten J J, Vieira D J and Zhao X 2001 Parity violation observed in the beta decay of magnetically trapped ^{82}rb atoms *Phys. Rev. Lett.* **86** 2967

[113] Feldbaum D, Wang H, Weinstein J, Vieira D and Zhao X 2007 Trapping radioactive ^{82}Rb in an optical dipole trap and evidence of spontaneous spin polarization *Phys. Rev.* A **76** 051402

[114] De Zafra R L 1960 Optical pumping *Am. J. Phys.* **28** 646

[115] Melconian D *et al* 2007 Measurement of the neutrino asymmetry in the β decay of laser-cooled, polarized ^{37}K *Phys. Lett.* B **649** 370

[116] Hallin A L, Calaprice F P, MacArthur D W, Piilonen L E, Schneider M B and Schreiber D F 1984 Test of time-reversal symmetry in the β Decay of ^{19}Ne *Phys. Rev. Lett.* **52** 337

[117] Soldner T, Beck L, Plonka C, Schreckenbach K and Zimmer O 2004 New limit on T violation in neutron decay *Phys. Lett.* B **581** 49
[118] Treiman S B 1957 Recoil effects in K capture and β decay *Phys. Rev.* **110** 448
[119] Pitcairn J R A *et al* 2009 Tensor interaction constraints from β decay recoil spin asymmetry of trapped atoms *Phys. Rev.* C **79** 015501
[120] Miller K W, Dürr S D and Wieman C E 2002 RF-induced Sisyphus colling in an optical dipole trap *Phys. Rev.* A **66** 023406
[121] Prime E J, Behr J A and Pearson M R 2007 Loading of a far off resonance dipole force trap for stable ^{39}K *Can. J. Phys.* **85** 1
[122] Gomez E, Orozco L A and Sprouse G D 2006 Spectroscopy with trapped francium: advances and perspectives for weak interaction studies *Rep. Prog. Phys.* **69** 79
[123] Fortson E N, Sandars P and Barr S 2003 The search for a permanent electric dipole moment *Phys. Today* **56** 33
[124] Pospelov M and Ritz A 2005 Electric dipole moments as probes of new physics *Ann. Phys.* **318** 119
[125] Sakharov A D 1967 Violation of CP invariance, C asymmetry, and baryon asymmetry of the universe *J. Exp. Theor. Phys.* **5** 24
[126] Auerbach N and Zelevinsky V 2008 Nuclear structure and the search for collective enhancement of P, T-violating Schiff moments *J. Phys. G: Nucl. Part. Phys.* **35** 093101
[127] Wilschut H W *et al* 2007 Status of the TRIμP project *Hyperfine Interact.* **174** 453
[128] Sakemi Y 2005 Feasibility test for permanent electric dipole search of francium atom— measurement of Francium yield produced from heavy-ion fusion reaction *Experimental proposal at RCNP*
Sakemi Y 2006 Search for permanent electric dipole moments of francium atom RIBF2006 *Int. Workshop on Nuclear Physics with RIBF, Riken, Japan*
[129] Amini J and Gould H 2003 High precision measurement of the static dipole polarizability of cesium *Phys. Rev. Lett.* **91** 153001
[130] Amini J M, Munger C T Jr and Gould H 2007 Electron electric-dipole-moment experiment using electric-field quantized slow cesium atoms *Phys. Rev.* A **75** 063416
[131] Lu Z-T, Corwin K L, Vogel K R, Wieman C E, Dinneen T P, Maddi J and Gould H 1997 Efficient Collection of 221Fr into a vapor cell magneto-optical trap *Phys. Rev. Lett.* **79** 994
[132] Byrnes T M, Dzuba V A, Flambaum V V and Murray D W 1999 Enhancement factor for the electron electric dipole moment in francium and gold atoms *Phys. Rev.* A **59** 3082
[133] Tardiff E R *et al* 2008 Polarization and relaxation rates of radon *Phys. Rev.* C **77** 052501
[134] Honda K, Takasu Y, Kuwamoto T, Kumakura M, Takahashi Y and Yabuzaki T 2002 Optical dipole force trapping of a fermion-boson mixture of ytterbium isotopes *Phys. Rev.* A **66** 021401
[135] Maruyama R, Wynar R H, Romalis M V, Andalkar A, Swallows M D, Pearson C E and Fortson E N 2003 Investigation of sub-Doppler cooling in an ytterbium magneto-optical trap *Phys. Rev.* A **68** 011403
[136] Bijlsma M, Verhaar B J and Heinzen D J 1994 Role of collisions in the search for an electron electric-dipole moment *Phys. Rev.* A **49** R4285
[137] Romalis M V and Fortson E N 1999 Zeeman frequency shifts in an optical dipole trap used to search for an electric-dipole moment *Phys. Rev.* A **59** 4547
[138] Natarajan V 2005 Proposed search for an electric-dipole moment using laser-cooled ^{171}Yb atoms *Eur. Phys. J.* D **32** 33
[139] Takeuchi M, Ichihara S, Takano T, Kumakura M and Takahashi Y 2007 Spin noise measurement with diamagnetic atoms *Phys. Rev.* A **75** 063827
[140] Choi J M and Cho D 2007 Elimination of inhomogeneous broadening for a ground-state hyperfine transition in an optical trap *J. Physics: Conf. Ser.* **80** 012037 (doi:10.1088/1742-6596/80/1/012037)
[141] Chin C, Leiber V, Vuletic V, Kerman A J and Chu S 2001 Measurement of an electron's electric dipole moment using Cs atoms trapped in optical lattices *Phys. Rev.* A **63** 033401
[142] Fang F and Weiss D 2007 Resonator-enhanced optical guiding and trapping of Cs atoms *Bull. Am. Phys. Soc.* **R1.00054** (DAMOP07 Calgary)
[143] Prescott C Y *et al* 1978 Parity non-conservation in inelastic electron scattering *Phys. Lett.* B **77** 347
[144] Prescott C Y *et al* 1979 Further measurements of parity non-conservation in inelastic electron scattering *Phys. Lett.* B **84** 524
[145] Haxton W C, Liu C-P and Ramsey-Musolf M J 2002 Nuclear anapole moments *Phys. Rev.* C **65** 045502
[146] Ramsey-Musolf M J and Page S A 2006 Hadronic parity violation: a new view through the looking glass *Ann. Rev. Nucl. Par. Sci.* **56** 1

[147] Vesna V A, Gledenov Yu M, Nesvizhevsky V V, Petoukhov A K, Sedyshev P V, Soldner T, Zimmer O and E V Shulgina E V 2008 Measurement of the parity-violating triton emission asymmetry in the reaction ^{6}Li(n,alpha)^{3}H with polarized cold neutrons *Phys. Rev.* C **77** 035501
[148] Prézeau G, Ramsey-Musolf M and Vogel P 2003 Neutrinoless double β decay and effective field theory *Phys. Rev.* D **68** 034016
[149] Gomez E, Aubin S, Sprouse G D, Orozco L A and DeMille D P 2007 Measurement method for the nuclear anapole moment of laser-trapped alkali-metal atoms *Phys. Rev.* A **75** 033418
[150] Loving C E and Sandars P G H 1977 On the feasibility of an atomic beam resonance experiment sensitive to the nuclear-spin-dependent weak neutral current interaction *J. Phys. B: At. Mol. Phys.* **10** 2755
[151] DeMille D, Cahn S B, Murphree D, Rahmlow D A and Kozlov M G 2008 Using molecules to measure nuclear spin-dependent parity violation *Phys. Rev. Lett.* **100** 023003
[152] Ezhov V F, Kozlov M G, Krygin G B, Ryzhov V A and Ryabov V L 2006 On the possibility of measuring the anapole moment of potassium atom *Tech. Phys. Lett.* **30** 917
[153] Porsev S G, Beloy K and Derevianko A 2009 Precise determination of electroweak coupling from atomic parity violation and implications for particle physics arXiv:0902.0335
[154] Stalnaker J E, Budker D, DeMille D P, Freedman S J and Yashchuk V V 2002 Measurement of the forbidden $6s2\,^{1}S_0 \rightarrow 5d6s\,^{3}D_1$ magnetic-dipole transition amplitude in atomic ytterbium *Phys. Rev.* A **66** 031403
[155] Bouchiat M-A 2007 Linear stark shift in dressed atoms as a signal to measure a nuclear anapole moment with a cold-atom fountain or interferometer *Phys. Rev. Lett.* **98** 043003
[156] Erler J and Ramsey-Musolf M J 2005 The weak mixing angle at low energies *Phys. Rev.* D **72** 073003
[157] Ramsey-Musolf M J and Su S 2008 Low energy precision test of supersymmetry *Phys. Rep.* **456** 1
[158] Young R D, Carlini R D, Thomas A W and Roche J 2007 Testing the Standard Model by precision measurement of the weak charges of quarks *Phys. Rev. Lett.* **99** 122003
[159] Langacker P 2008 The Physics of heavy Z' gauge bosons *Ann. Rev. Nucl. Part. Sci.* (arXiv:0801.1345) submitted
[160] Bouchiat C and Fayet P 2005 Constraints on the parity-violating couplings of a new gauge boson *Phys. Lett.* B **608** 87
[161] Dunford R W and Holt R J 2007 Parity violation in hydrogen revisited *J. Phys. G: Nucl. Part. Phys.* **34** 2099
[162] Bouchiat M-A and Bouchiat C 2001 An atomic linear Stark shift violating P but not T arising from the electroweak nuclear anapole moment *Eur. Phys. J.* D **15** 5
[163] Wood C S, Bennett S C, Cho D, Masterson B, Roberts J L, Tanner C E and Wieman C E 1997 Measurement of parity nonconservation and an anapole moment in cesium *Science* **275** 1759
[164] Wood C S, Bennett S C, Roberts J L, Cho D and Wieman C E 1999 Precision measurement of parity violation in cesium *Can. J. Phys.* **77** 7
[165] Guéna J, Lintz M and Bouchiat M-A 2005 Measurement of the parity violating 6S-7S transition amplitude in cesium achieved withing 2×10^{-13} atomic-unit accuracy by stimulated-emission detection *Phys. Rev.* A **71** 042108
[166] Sanguinetti S, Guéna J, Lintz M, Jacquier Ph, Wasan A and Bouchiat M-A 2003 Prospects for forbidden-transition spectroscopy and parity violation measurements using a beam of cold stable or radioactive atoms *Eur. Phys. J.* D **25** 3
[167] Bouchiat M-A 2008 Measuring the Fr weak nuclear charge by observing a linear Stark shift with small atomic samples *Phys. Rev. Lett.* **100** 123003
[168] Koerber T W, Schacht M, Nagourney W and Fortson E N 2003 Radio frequency spectroscopy with a trapped Ba^{+} ion: recent progress and prospects for measuring parity violation *J. Phys. B: At. Mol. Opt. Phys.* **36** 637
[169] Sahoo B K, Das B P, Chaudhuri R K, Mukherjee E, Timmermans R G E and Jungmann K 2007 Investigations of Ra^{+} properties to test possibilities for new optical-frequency standards *Phys. Rev.* A **76** 040504
[170] Stancari G *et al* 2007 Francium sources and traps for fundamental interaction studies *Euro. Phys. J.* **150** 389
[171] Atutov S N *et al* 2003 Fast and efficient loading of a Rb magneto-optical trap using light-induced atomic desorption *Phys Rev.* A **67** 053401
[172] Savukov I M, Derevianko A, Berry H G and Johnson W R 1999 Large contributions of negative-energy states to forbidden magnetic-dipole transition amplitudes in alkali-metal atoms *Phys. Rev. Lett.* **83** 2914
[173] Dzuba V A, Flambaum V V and Safronova M S 2006 Breit interaction and parity nonconservation in many-electron atoms *Phys. Rev.* A **73** 022112
[174] Vieira D J and Wieman C E 1992 Parity nonconservation measurements of trapped radioactive isotopes—a precise test of the Standard Model *Technical report, Los Alamos*
[175] Horowitz C J, Pollock S J, Souder P A and Michaels R 2001 Parity violating measurements of neutron densities *Phys. Rev.* C **63** 025501

[176] Sil Tapas, Centelles M, Viñas X and Piekarewicz J 2005 Atomic parity nonconservation, neutron radii, and effective field theories of nuclei *Phys. Rev.* C **71** 045502

[177] Brown B A, Derevianko A and Flambaum V V 2008 Dispelling the curse of the neutron skin in atomic parity violation arXiv:0804.4315v1

[178] Grossman J S, Orozco L A, Pearson M R, Simsarian J E, Sprouse G D and Zhao W Z 1999 Hyperfine anomaly measurements in francium isotopes and the radial distribution of neutrons *Phys. Rev. Lett.* **83** 935

[179] Pearson M R (spokesperson) Hyperfine anomaly measurements in neutron deficient francium isotopes, TRIUMF experiment S1010, http://www.triumf.info/facility/experimenters/expdb/public.php